



A new pale-ventered nurse frog (Aromobatidae: *Allobates*) from southwestern Brazilian Amazonia

Jesus R. D. Souza^{1,2}, Miquéias Ferrão^{1,3}, Igor Luis Kaefer¹, Antonio Saulo Cunha-Machado⁴, Paulo Roberto Melo-Sampaio⁵, James Hanken³, Albertina Pimentel Lima⁴

¹ Programa de Pós-Graduação em Zoologia, Universidade Federal do Amazonas, Manaus, Amazonas, Brazil

² Instituto de Meio Ambiente do Acre, Rio Branco, Acre, Brazil

³ Museum of Comparative Zoology, Harvard University, Cambridge, Massachusetts, United States of America

⁴ Coordenação de Biodiversidade, Instituto Nacional de Pesquisas da Amazônia, Manaus, Amazonas, Brazil

⁵ Departamento de Vertebrados, Museu Nacional, Rio de Janeiro, Rio de Janeiro, Brazil

<https://zoobank.org/D1F9510F-919B-43F1-AEE4-1B8b6C1113D9>

Corresponding author: Miquéias Ferrão (uranoscodon@gmail.com)

Academic editor Raffael Ernst

Received 15 March 2023

Accepted 5 June 2023

Published 21 July 2023

Citation: Souza JRD, Ferrão M, Kaefer IL, Cunha-Machado AS, Melo-Sampaio PR, Hanken J, Lima AP (2023) A new pale-ventered nurse frog (*Aromobatidae: Allobates*) from southwestern Brazilian Amazonia. *Vertebrate Zoology* 73 647–675. <https://doi.org/10.3897/vz.73.e103534>

Abstract

We use integrative taxonomy to formally describe a candidate species of nurse frog of the genus *Allobates* from southwestern Brazilian Amazonia. The new species nests within a clade that has been defined historically as *A. gasconi*, but it has an 8.8–11.0% genetic distance for 16S to samples from the type locality of *A. gasconi*. The new species differs from congeners mainly by males having a translucent white throat and vocal sac; advertisement calls with a duration of 42–60 ms, two notes separated by an inter-note interval of 8–23 ms, and a dominant frequency of 4,953–6,331 Hz; and exotrophic tadpoles with 2 pyramidal papillae on each end of the upper lip and 10–13 pyramidal and cylindrical papillae surrounding the lower lip. Phylogenetic analyses based on mitochondrial DNA suggest that *A. gasconi* sensu lato as defined previously represents a complex of as many as seven species, corroborating studies that have shown high levels of cryptic diversity within *Allobates*.

Keywords

Advertisement call, biodiversity, integrative taxonomy, morphology, phylogeny, reproductive behavior, State of Acre, tadpole

Introduction

Nurse frogs of the genus *Allobates* Zimmermann & Zimmermann, 1988 are leaf-litter inhabitants of neotropical forests distributed from Central America to the east coast of South America (Grant et al. 2006, 2017; Frost 2023). Diverse reproductive behavior among species is associated with several different reproductive modes (sensu Nunes-de-Almeida et al. 2021), with most species depositing eggs on leaf-litter (e.g., *A. caldwella* and *A. tapajós*; Lima et al. 2015, 2020) but others depositing them on

the adaxial (e.g., *A. carajas* and *A. velocicantus*; Simões et al. 2019; Souza et al. 2020) or abaxial (e.g., *A. subfolionidificans*; Lima et al. 2007) surface of live leaves of small shrubs. Clutch size varies among species, as does coloration of eggs and the surrounding jelly (Lima et al. 2020). Parental care is common to all *Allobates*; species with exotrophic, free-swimming tadpoles exhibit clutch care and tadpole transport (e.g., *A. femoralis*), while species with endotrophic terrestrial tadpoles exhibit only

clutch care (e.g., *A. nidicola*, *A. masniger*; Caldwell and Lima 2003).

Advertisement calls may be classified into two main types following the note-centered approach (sensu Köhler et al. 2017): Those with two or more notes (e.g., *A. flaviventris* and *A. trilineatus*; Melo-Sampaio et al. 2013; Jaramillo et al. 2021) and those with a single note (e.g., *A. nidicola* and *A. paleovarzensis*; Caldwell and Lima 2003; Lima et al. 2010). Most species are cryptically colored and exhibit little morphological divergence, which contrasts sharply with extensive genetic, behavioral and bioacoustic divergence that characterizes most interspecific comparisons (Kaefer et al. 2013; Maia et al. 2017; Fernandes et al. 2021).

The recent increase in the understanding of taxonomic diversity of *Allobates* is impressive: at least thirteen species have been described in just the last five years (Melo-Sampaio et al. 2018, 2020; Simões et al. 2018, 2019; Moraes et al. 2019; Lima et al. 2020; Souza et al. 2020; Gagliardi-Urrutia et al. 2021; Moraes and Lima 2021; Silva et al. 2022; Ferrão et al. 2022; Fouquet et al. 2023). This trend may be attributed to the increased sampling of remote areas of Amazonia and to the use of integrative taxonomy (e.g., Simões et al. 2018, 2019; Lima et al. 2020; Souza et al. 2020; Silva et al. 2022). These advances in alpha taxonomy and sampling coverage have led to new biogeographic hypotheses about the origin and diversification of this diverse genus (e.g., Réjaud et al. 2020). Nevertheless, many studies have concluded that species diversity in *Allobates* remains underestimated and that, in particular, some widely distributed species (e.g., *A. gasconi*, *A. granti*, *A. tapajos*, *A. tinae* and *A. trilineatus*) likely represent complexes of multiple species, each with a more restricted geographic distribution (Lima et al. 2020; Vacher et al. 2020; Jaramillo et al. 2021; Ferrão et al. 2022; Fouquet et al. 2023).

Allobates gasconi was described based on the morphology of 33 individuals from five localities along both banks of the Juruá River, southwestern Brazilian Amazonia (Moraes 2002). Several subsequent studies published genetic sequences tentatively identified as *A. gasconi*. Grant et al. (2006) published the first phylogenetic inference that included *A. gasconi*, based on individuals collected from the Ituxi River, an eastern tributary of the upper Purus River and ~400 km from the type locality in the Juruá River. Santos et al. (2009) subsequently applied the name *A. gasconi* to individuals from Porto Walter in the upper Juruá River (Acre, Brazil), which were recently assigned to *A. trilineatus* (Melo-Sampaio et al. 2018). Lima et al. (2014) sequenced individuals from the middle Juruá River (Eirunepé, Amazonas, Brazil) and identified them as *A. gasconi*. Melo-Sampaio et al. (2018) compiled these molecular data, corrected misidentifications and sequenced new samples from several localities in the upper Juruá and Purus basins (Acre and Amazonas, Brazil), recovering three deeply diverging mtDNA lineages within *A. gasconi* sensu lato. More recently, Vacher et al. (2020) sequenced new individuals of *A. gasconi* from the upper Madeira River (Rondônia, Brazil) and showed the existence of at least three highly distinct mtDNA lineages. However, their

analysis did not include the newly sequenced individuals reported by Melo-Sampaio et al. (2018) from Acre. Réjaud et al. (2020) delimited all these lineages as a single species and recovered it as a member of the *A. caeruleodactylus* clade. Recently, Ferreira et al. (2023) redescribed *A. gasconi* based on fresh material from type and paratype localities and showed that none of those individuals identified as *A. gasconi* in earlier studies indeed represents *A. gasconi* sensu stricto. Moreover, Ferreira et al. (2023) highlighted that *A. gasconi* sensu lato comprises at least three candidate species and that none is closely related phylogenetically to *A. gasconi* sensu stricto.

We recently surveyed multiple localities in southwestern Amazonia (Acre, Brazil). Among the material collected are several individuals of *Allobates gasconi* sensu lato that nest within a previously reported lineage by Melo-Sampaio et al. (2018) and Ferreira et al. (2023). In this study, we describe them as a new species based on morphological, bioacoustic, and molecular data, as well as their breeding behavior.

Materials and methods

Sampling

Adult individuals were collected between November 2018 and February 2020 from five localities in southwestern Brazilian Amazonia—four in the State of Acre (forest fragment near the BR 364 highway, municipality of Manoel Urbano [8°52'27"S, 69°17'07"W, 166 meters above sea level—hereafter m asl]; east bank of the Antimary River, municipality of Bujari [09°29'16"S, 68°21'20"W, 168 m asl]; Parque Ambiental Chico Mendes, municipality of Rio Branco [10°02'13"S, 67°47'36"W, 158 m asl]; and municipality of Feijó [08°14'13"S, 70°22'44"W, 184 m asl]) and a fifth in the State of Amazonas (Reserva Extrativista Arapixi, municipality of Boca do Acre [08°58'21"S, 67°51'50"W, 125 m asl]). Ten tadpoles (INPAH45066) were taken from the dorsum of a male (INPAH45045) collected in Manoel Urbano on January 18, 2020; 18 eggs were taken from a freshly laid spawn (field number APL21511b) on January 7, 2020.

Tadpoles and eggs were reared in the laboratory until they reached Gosner (1960) developmental stages 33–37. Adults were killed with 2% aqueous benzocaine, fixed in 10% neutral-buffered formalin (NBF), and preserved in 70% ethanol. Tadpoles were killed with 2% aqueous benzocaine diluted in water and fixed in 10% NBF. Tissue samples for genetic analysis were removed before fixation and stored in 95% ethanol. Adults and tadpoles are deposited in herpetological collections at the Museu de Ciências e Tecnologia da Pontifícia Universidade Católica do Rio Grande do Sul (MCP; Porto Alegre, Brazil), Instituto Nacional de Pesquisas da Amazônia (INPAH; Manaus, Brazil), Museu Nacional (MNRJ; Rio de Janeiro, Brazil) and Museu Paraense Emílio Goeldi (MPEG; Belém, Brazil).

Advertisement calls of 17 males were recorded: eight from Manoel Urbano, two from Antimary River, three from Parque Ambiental Chico Mendes, one from Feijó and three from Reserva Extrativista Arapixi. Recordings were made between 0630 and 1100 h and between 1500 and 1730 h using a Sony PCM-D50 digital recorder with built-in microphone, a CSR Yoga HT-81 Shotgun directional microphone attached to a Zoom H4n recorder, and a Sennheiser ME 66 unidirectional microphone attached to a Marantz PMD661 digital recorder. Microphones were positioned approximately 1 m from the focal male. Recordings were taken at 16-bit resolution and 44.1 kHz and stored in WAV format. Air temperature recorded at the time of recordings ranged from 21 to 29°C. Recordings are deposited in the Fonoteca Neotropical Jacques Vielliard (FNJV 53680–93), UNICAMP, Campinas, Brazil.

Sequencing and phylogenetic analysis

Total genomic DNA was extracted from tissue samples of five individuals of the new species from Manoel Urbano, two from Antimary River and two from Parque Ambiental Chico Mendes (Rio Branco). DNA extractions were obtained using the commercial kit Wizard (Promega Corp., Madison, WI, USA) following manufacturer's instructions. Fragments of the 16S rRNA mitochondrial gene were amplified by polymerase chain reaction (PCR) using the universal primers 16sar (CGCCTGTTTATCAAAAACAT) and 16sbr (CCGGTCTGAACTCAGATCACGT; Palumbi 1996). The PCR with final volume of 15 µL contained 6.4 µL distilled and deionized water; 1.5 µL MgCl₂ (25 mM); 1.5 µL Tris-HCl buffer (10 mM); 1.5 µL dNTPs (25 mM); 1.5 µL 16sar primer at 2 pmol/µL; 1.5 µL 16sbr primer at 2 pmol/µL; 0.1 µL taq DNA polymerase (5 U/µL); and 1 µL DNA (10 ng/µL). The following thermocycling process was used for amplifying the reaction: 92°C for 30 s for the initial denaturation, 35 cycles of denaturation at a temperature of 92°C for 10 s, annealing at 50°C for 35 s, and extension at 72°C for 90 s; the final extension was performed at 72°C for 10 min. PCR products were purified with PEG (polyethylene glycol) 8000 and sequenced using the Big Dye Terminator Kit (Applied Biosystems, Waltham, USA) in an automated sequencer ABI Prism 3130 (ThermoFisher Scientific, Waltham, USA). Sequences were visually checked and manually edited in GENEIOUS 5.3.4 (Kearse et al. 2012). Newly generated sequences are deposited in GenBank (<http://www.ncbi.nlm.nih.gov/Genbank>) under accession numbers ON937745–53.

Sequences of the 16S fragment and four additional genes (12S ribosomal RNA [12S], cytochrome c oxidase I [COI], cytochrome B [cyt *b*] and NADH dehydrogenase 1 [ND1]) were retrieved from GenBank to infer the phylogenetic relationship of the new species, including sequences of five individuals of the new species previously reported as *A. gasconi* by Melo-Sampaio et al. (2018). Sequences of *Ameerega* Bauer, 1986, *Anomaloglossus* Grant et al., 2006, *Aromobates* Myers et al., 1991, *Co-*

lostethus Cope, 1866, *Dendrobates* Wagler, 1830, *Leucostethus* Grant et al., 2017, *Mannophryne* La Marca, 1992, *Phyllobates* Bibron, 1840, *Rheobates* Grant et al., 2006 and *Silverstoneia* Grant et al., 2006 were used as outgroups. The final dataset combined 104 sequences of 16S, 60 of 12S, 50 of COI, 64 of cyt *b* and 41 of ND1. Sequences were aligned separately for each gene with the online implementation of the MAFFT algorithm (<https://mafft.cbrc.jp>) using the E-INS-i strategy for RNA genes and G-INS-i for the protein-coding genes (Katoh and Standley 2013). MESQUITE 3.04 (Maddison and Maddison 2015) was used to concatenate alignments and generate the final matrix, which is composed of 6,251 base-pairs and 104 terminals. Appendix 1 lists vouchers and GenBank accession numbers for the entire dataset.

The final matrix was split into 10 partitions, one for RNA genes (12S plus 16S) and one for each codon of protein-coding genes (COI, cyt *b* and ND1). The following best-fit partitioning scheme and nucleotide models were inferred with MODELFINDER (Kalyaanamoorthy et al. 2017) implemented in IQ-TREE (Nguyen et al. 2015): GTR+F+R6 for 12S+16S, SYM+I+G4 for cyt *b* 1st codon plus ND1 1st codon, TIM+F+I+G4 for cyt *b* 2nd codon plus ND1 2nd codon plus COI 2nd codon, TN+F+R5 for cyt *b* 3rd codon plus ND1 3rd codon plus COI 3rd codon, and TIM3e+I+G4 for COI 1st codon. Phylogenetic relationship was inferred through Maximum Likelihood inference using IQ-TREE. Node support was calculated using 10,000 ultrafast bootstrap approximation replicates (Hoang et al. 2018) with a maximum 10,000 iterations (unsuccessful iterations to stop > 100), a 0.99 minimum correlation coefficient and 10,000 replicates of the Shimodaira-Hasegawa approximate likelihood ratio test (SH-aLRT). Uncorrected (p) and Kimura-2-parameter (K2p) distances (Kimura 1980) between the new species and other nurse frogs were calculated with MEGA 11 (Tamura et al. 2021).

Molecular species delimitation

We conducted three molecular species delimitation analyses to delimit putative species: Generalized Mixed Yule Coalescent (GMYC; Pons et al. 2006; Fujisawa and Barraclough 2013), Assemble Species by Automatic Partitioning (ASAP; Puillandre et al. 2021) and Automatic Barcode Gap Discovery (ABGD; Puillandre et al. 2012). GMYC delimits putative species by optimizing the set of nodes that define the transitions between inter- and intra-specific processes through speciation (Yule 1925) and neutral coalescent (Hudson 1990) models (Pons et al. 2006; Fujisawa and Barraclough 2013). ASAP and ABGD are clustering algorithms that implement pairwise genetic distances (Jukes-Cantor, K2P or p distances) to estimate multiple potential barcode gaps and define minimum distance thresholds to partition samples into putative species. The main difference between them is that the best partition is selected through a score system in ASAP, while in ABGD this selection is unsupervised and based on prior knowledge regarding interspecific genetic

distance thresholds. As delimitations may differ between methods, a lineage was considered a candidate species if it was supported by at least two methods (majority rule consensus).

Molecular species delimitation analyses were conducted with the complete 16S alignment, which include all other species of *Allobates* included in previous phylogenetic analyses. GMYC requires a single-locus ultrametric phylogenetic tree as input, therefore a 16S tree was inferred through Bayesian Inference in BEAST 2.6.3 (Bouckaert et al. 2019) using a relaxed log-normal clock model and Yule Process tree prior; a run of 100 million generations was sampled every 10,000 steps. Stationarity and effective sample size (> 200) of posterior distributions and priors were checked in TRACER v1.7.1 (Rambaut et al. 2018). The Maximum Clade Credibility (MCC) tree was annotated using TREEANOTATOR v.2.6.3 (Bouckaert et al. 2019) after burn-in of 40%. The GMYC was run in the webserver <https://species.h-its.org/gmyc> using the single threshold. ASAP was run in the webserver <https://bioinfo.mnhn.fr/abi/public/asap> using p distances as the substitution model and default parameters. ABGD was run in the webserver <https://bioinfo.mnhn.fr/abi/public/abgd> using p distances as the sequence substitution model, minimum intraspecific pairwise distance = 0.001 and maximum = 0.1, 10 iterative steps, and relative gap width (X) = 1. ASAP and ABGD were run with the 16S alignment.

Morphological characters

Sex was determined by the presence of a vocal sac or direct observation of vocal activity in males, and by the presence of eggs (visible through belly skin) in females. The following linear measurements, taken using a digital calipers (precision 0.01 mm) or a stereomicroscope (precision greater than 0.1 mm), follow Lima et al. (2007): Snout-vent length (SVL); head length (HL); interorbital distance (IO); head width (HW); snout length (SL); eye-nostril distance (END); inter-nostril distance (IND); eye length (EL); tympanic diameter (TYM); forearm length (FAL); upper arm length (UAL); thigh length (THL); tibia length (TIL); foot length (FL); hand length from the proximal edge of the palmar tubercle to the tip of finger I (HANDI), finger II (HANDII), finger III (HANDIII) and finger IV (HANDIV); width of finger III disc (WFD); palmar tubercle diameter (DPT); width of thenar tubercle (WTT); width of finger III at proximal phalanx (WPF); and width of toe IV disc (WTD). Terminology and morphological characters follow Grant et al. (2017), except for finger numbering (I–IV). Character states of swelling on finger III follow Cavalcanti et al. (2022). Morphological descriptions follow Souza et al. (2020). Coloration is described from photographs and fieldnotes. Coloration is described from photos of formalin-fixed specimens. Morphometric measurements are listed in Table S1.

Developmental stage was scored according to Gosner (1960). Twelve tadpoles were measured from lot INPAH45066, all at stages 34–37. The following lin-

ear measurements, taken with a micrometer coupled to a stereomicroscope, follow Altig and McDiarmid (1999), Schulze et al. (2015) and Randrianiaina et al. (2011): Total length (TL); body length (BL); tail length (TAL); body width (BW); body height (BH); head width (HWLE); tail muscle width (TMW); maximum tail height (MTH); tail muscle height (TMH); interorbital distance (IOD); inter-nostril distance (IND); eye-nostril distance (END); nostril-snout distance (NSD); eye diameter (ED); vent-tube length (VTL); spiracle-tube length (STL); snout-spiracle distance (SS); oral-disc width (ODW); size of the anterior gap of marginal papillae (DG); upper jaw width (UJW); upper jaw length (UJL); posterior (PL) and anterior (AL) labium length; width of the first (A1) and second (A2) anterior keratodont row; and width of the first (P1), second (P2) and third (P3) posterior keratodont rows. Terminology and diagnostic characters follow Altig and McDiarmid (1999) and Schulze et al. (2015). Characterization of body shape follows Dubeux et al. (2020). Morphological descriptions are based on six tadpoles at stage 34 and follow Schulze et al. (2015). Coloration is described from photos of formalin-fixed specimens. Morphometric measurements are listed in Table S2.

Morphological analysis

Ferreira et al. (2023) show that *Allobates gasconi* sensu stricto and the new species (as *A. gasconi* SL4) are not closely related. However, they have been misidentified historically. Due to that, we also took the above morphometric measurements from topotypic adults of *A. gasconi* recently collected by Ferreira et al. (2023) to allow direct comparisons between them and adults of the new species. The type series of *A. gasconi* is considerably dehydrated (Ferreira et al. 2023). To avoid biasing the statistical analysis with potentially confounding data, we did not use type specimens.

Although body size may be informative in some interspecific pair-wise comparisons, statistical artifacts are eventually associated with the use of raw body ratios (all measurements against SVL) in standard Principal Component Analysis (PCA), thus we ran an adapted PCA called Shape PCA (Baur and Leuenberger 2011). Briefly, raw morphometric measurements are first log-transformed and then standardized using log-mean of each variable to avoid nonlinearity issues. Then, size and shape algorithms are implemented to allow the interpretation of principal components (PC) in terms of body shape and isometric size (isozize). Isozize is the geometric mean of all morphometric measurements of an individual (Baur and Leuenberger 2011). Shape PCA was run separately for males and females using the R script available at Zenodo (DOI: 10.5281/zenodo.3890195; Baur and Leuenberger 2020). To test if body shape and isozize of *A. gasconi* sensu stricto differ statistically from those of the new species, one-way analysis of variance (one-way ANOVA) was run separately for shape PC1, shape PC2 and isozize, setting them as response variables and species as factors.

Statistical significance was calculated through Tukey's test using $\alpha = 0.05$. Morphometric measurements of both species are available at Table S1.

Presence of sexual dimorphism in SVL and 22 morphometric ratios of the new species was evaluated with one-way ANOVAs through the function `aov` of the package `stats` (R Core Team 2021). Homogeneity of variances was checked visually with Residuals vs. Fitted values Plot and tested with Levene test using the function `leveneTest` of the `car` package (Fox and Weisberg 2019). Normality of residuals was inspected with Normal Q-Q plots and tested with the Shapiro-Wilk test through the function `shapiro.test` of the `stats` package. Outliers were excluded from analyses to fit homogeneity and normality assumptions. Multiple comparisons adjustment of p values was calculated using Benjamini and Hochberg correction (Benjamini and Hochberg 1995) through the function `p.adjust` of the package `stats`.

Bioacoustic analysis

Terminology used to describe the advertisement call of the new species follows the note-centered approach (Köhler et al. 2017). The following spectral and temporal parameters were measured from ten calls of 17 males:

call duration (CD), inter-call interval (ICI), call-series duration (CSD), inter-call-series interval (ICSI), note duration measured in the first (ND1) and second (ND2) notes, inter-note interval (INI), lower (LFN1, LFN2), upper (HFN1, HFN2) and dominant (DFN1, DFN2) frequency of the first and second notes, respectively. All recordings were visually inspected to count the proportion of each call arrangement in the vocalization of the new species. Acoustic analyses were performed in Raven pro 1.5 (Bioacoustics Research Program 2015) set as follows: window = Blackman, Discrete Fourier Transform = 2,048 samples and 3 dB filter bandwidth = 80.0 Hz. Dominant frequency was measured using the Peak frequency function; upper and lower frequencies were measured 20 dB below the peak frequency to avoid background noise interference. Graphical representation of calls was generated in R using the Seewave package (Sueur et al. 2008) configured as follows: Hanning window, overlap of 85% and 256 points of resolution (FFT).

Breeding behavior

Notes on reproductive behavior were obtained from observation of four courtship events that occurred between 0600 and 0900 h: one in Manoel Urbano on February 7,

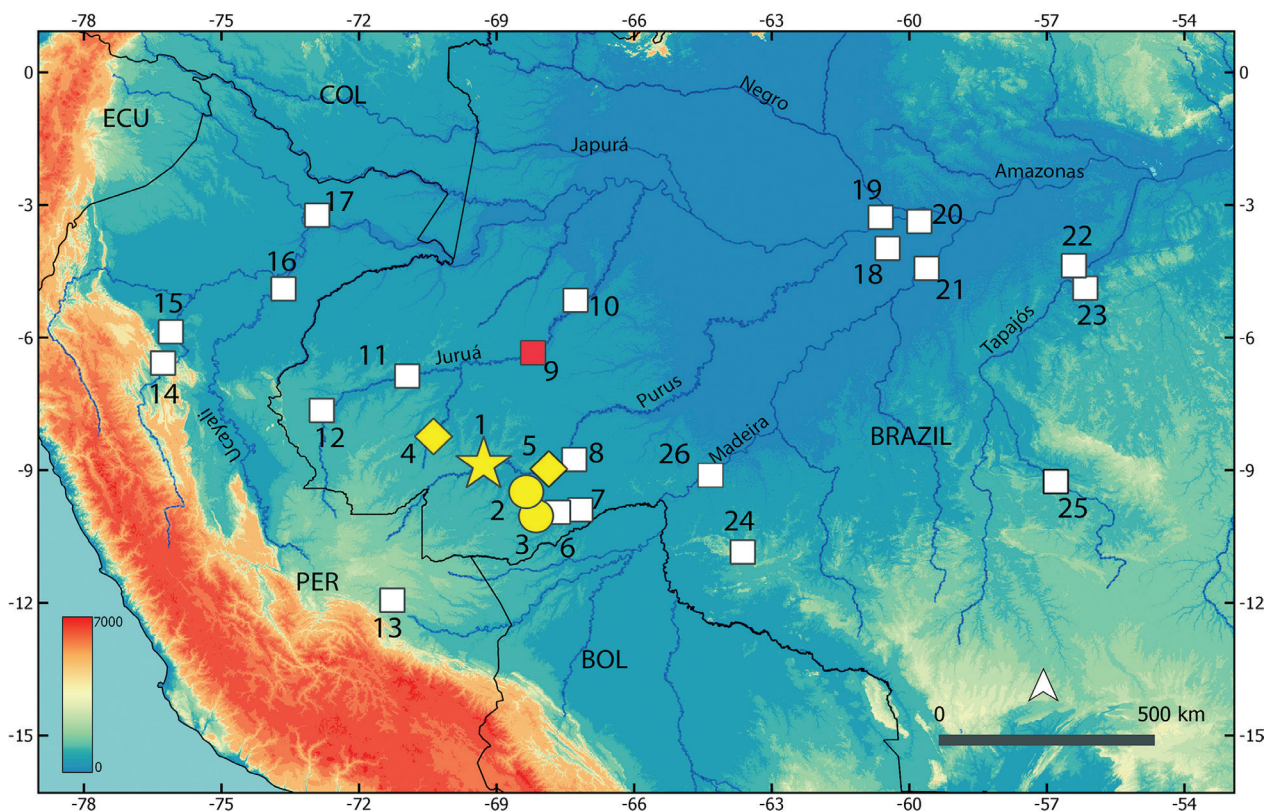


Figure 1. Geographic distribution of the new species (yellow symbols): Type locality = star (1 Manoel Urbano), paratype localities = circles (2 Antimary River; 3 Parque Ambiental Chico Mendes) and additional localities = rhombus (4, Feijó; 5, Reserva Extrativista Arapixi). Type localities of other *Allobates* to which it is compared (squares): 6 *A. subfolionidificans*; 7 *A. flaviventris*; 8 *A. tinae*; 9 *A. gasconi* (red square); 10 *A. vanzolinus*; 11 *A. fuscillus*; 12 *A. velocitans*; 13 *A. conspicuus*; 14 *A. ornatus*; 15 *A. trilineatus*; 16 *A. sieggreenae*; 17 *A. melanolaemus*; 18 *A. caeruleodactylus*; 19 *A. nidicola*; 20 *A. paleovarzensis*; 21 *A. grillisimilis*; 22 *A. tapajós*; 23 *A. grillicantus*; 24 *A. pacaas*; 25 *A. paleci*; 26 *A. kamilae*. Abbreviations: BOL, Bolivia; COL, Colombia; ECU, Ecuador; PER, Peru.

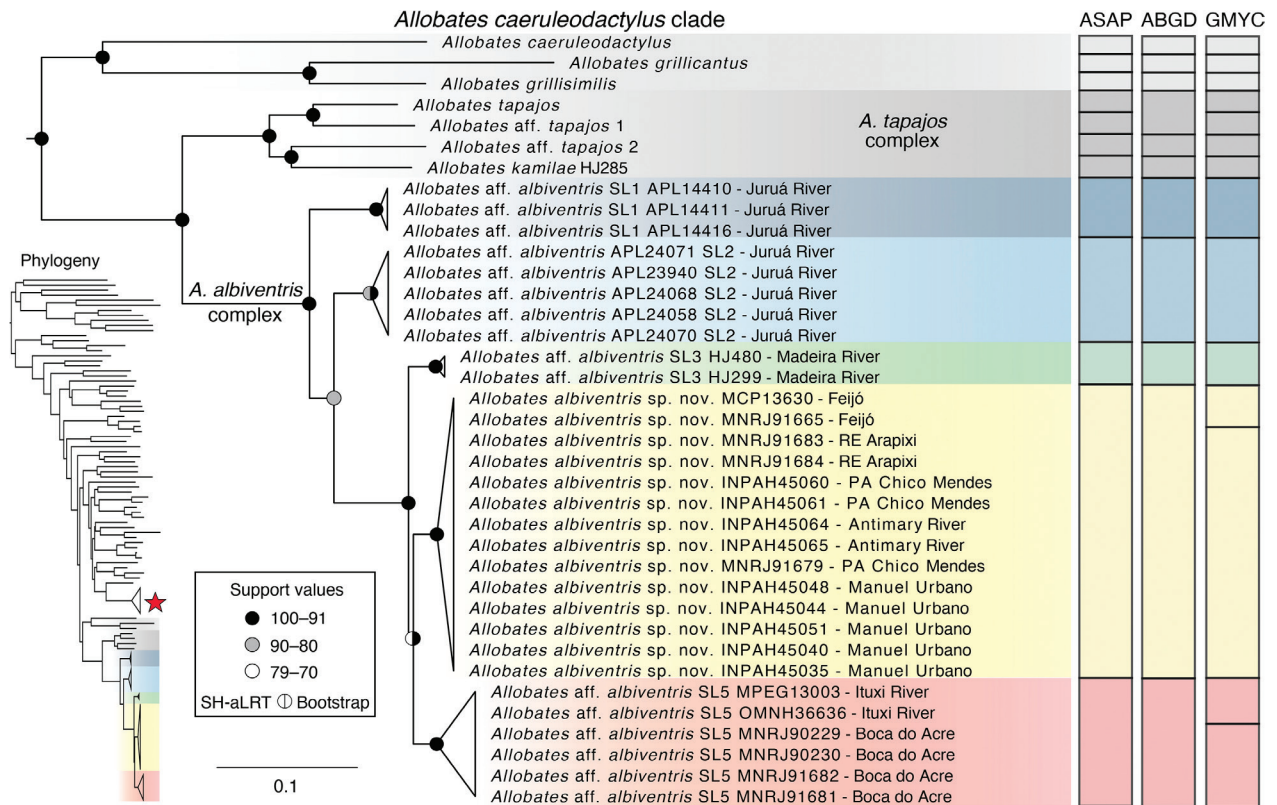


Figure 2. Phylogeny of *Allobates* based on five mitochondrial genes (12S, 16S, COI, cyt *b* and ND1), focusing on relationships within the *Allobates caeruleodactylus* clade. Node support was calculated following 10,000 ultrafast bootstrap approximation replicates and 10,000 replicates of the SH-aLRT branch test. Vertical bars represent species delimited with 16S through Automatic Barcode Gap Discovery (ABGD), Assemble Species by Automatic Partitioning (ASAP) and Generalized Mixed Yule Coalescent (GMYC) methods. The phylogenetic tree inset at lower left indicates the location of the *A. caeruleodactylus* clade in the overall *Allobates* phylogeny (Supplemental Figure 1). Red star in the compressed phylogeny represents *A. gasconi* sensu stricto. Note that individuals of *A. albiventris* sp. nov. and *A. aff. albiventris* were reported as *A. gasconi* in previous studies.

2020; the other three in Parque Ambiental Chico Mendes on February 12, 14 and 15, 2020. The courting male INPAH45044 and female INPAH45050 were collected; both are included in the type series.

Interspecific comparisons

The new species has been found only in the upper Juruá and Purus basins, southwestern Brazilian Amazonia. Since most *Allobates* have restricted geographic distributions when compared to species in other genera, interspecific comparisons here are limited to cryptically colored species known to be distributed in the southwestern Amazonian lowlands of Bolivia, Brazil and Peru (Appendix 2): *A. conspicuus* (Morales, 2002); *A. flaviventris* Melo-Sampaio, Souza & Peloso, 2013; *A. fuscillus* (Morales, 2002); *A. gasconi* (Morales, 2002); *A. kamillae* Ferrão, Hanken & Lima, 2022; *A. melanolaemus* (Grant & Rodríguez, 2001); *A. nidicola* (Caldwell & Lima, 2003); *A. ornatus* (Morales, 2002); *A. pacaas* Melo-Sampaio et al., 2020; *A. paleovarzensis* Lima, Caldwell, Biavati & Montanarin, 2010; *A. sieggreenae* Gagliardi-Urrutia et al., 2021; *A. subfolionidificans* (Lima, Sanchez & Souza, 2007); *A. tinae* Melo-Sampaio, Oliveira & Prates, 2018; *A. trilineatus* (Boulenger, 1884); *A. vanzolinus* (Morales, 2002);

and *A. velocicantus* Souza, Ferrão, Hanken & Lima, 2020. In addition, we make comparisons to species of the *A. caeruleodactylus* clade (sensu Réjaud et al. 2020): *A. caeruleodactylus* Lima & Caldwell, 2001; *A. grillisimilis* Simões, Sturaro, Peloso & Lima, 2013a; *A. grillicantus* Moraes & Lima, 2021; *A. paleci* Silva, Marques, Folly & Santana, 2022; and *A. tapajos* Lima, Simões & Kaefer, 2015. Corresponding type localities are plotted in Fig. 1.

Results

Phylogenetic relationships

The topology of our molecular phylogeny is consistent with that recovered in the most recently published phylogeny of *Allobates* (Réjaud et al. 2020), particularly with respect to the relationships among major clades (Figure S1). Three major clades compose the *A. caeruleodactylus* clade (Fig. 2): one grouping *A. caeruleodactylus*, *A. grillicantus* and *A. grillisimilis*; another one nesting members of the *A. tapajos* species complex; and the last one grouping species previously misidentified with *A. gasconi*. The last two clades are recovered as sisters with high support.

Table 1. Pairwise genetic distances between and within *Allobates gasconi* sensu stricto (SS) and species of the *Allobates albiventris* species complex based on a fragment of 16S rRNA. Uncorrected pairwise distances (p distance) and Kimura 2-parameter distances (K2P) are below and above the diagonal, respectively. Numbers in bold along the diagonal denote intraspecific p distances. Distances are expressed as percentage and presented as mean and range.

Species		1	2	3	4	5	6
1	<i>A. gasconi</i> SS	0.4 (0.0–0.9)	10.2 (9.0–12.1)	9.6 (8.8–11.0)	10.2 (9.0–11.8)	10.9 (9.5–12.3)	10.7 (9.3–12.6)
2	<i>A. aff. albiventris</i> SL1	9.5 (8.4–11.1)	0.1 (0.0–0.2)	3.1 (2.8–3.3)	4.8 (4.6–5.0)	4.1 (3.8–5.0)	4.5 (4.0–5.0)
3	<i>A. aff. albiventris</i> SL2	9.0 (8.3–10.1)	3.0 (2.8–3.2)	0.2 (0.0–0.6)	3.8 (3.7–4.1)	3.3 (2.8–4.3)	3.9 (3.5–4.4)
4	<i>A. aff. albiventris</i> SL3	9.5 (8.5–10.8)	4.6 (4.4–4.8)	3.7 (3.6–3.9)	0.2 (0.0–0.4)	1.9 (1.6–2.2)	2.3 (1.7–2.9)
5	<i>A. albiventris</i> sp. nov.	10.0 (8.8–11.0)	4.0 (3.8–4.8)	3.2 (2.9–4.1)	1.9 (1.6–2.1)	0.2 (0.0–0.4)	2.0 (1.2–2.5)
6	<i>A. aff. albiventris</i> SL5	9.9 (8.7–11.4)	4.3 (3.8–4.8)	3.7 (3.4–4.2)	2.2 (1.7–2.8)	2.0 (1.2–2.4)	0.6 (0.0–1.6)

The new species (*A. albiventris* sp. nov.) nests within the species complex that groups species previously misidentified as *Allobates gasconi*, which is called *A. albiventris* species complex hereafter. See Appendix 3 for geographic distribution of the *A. albiventris* species complex.

Within the species complex that groups species previously misidentified as *Allobates gasconi*, newly sequenced individuals of the new species (*A. albiventris* sp. nov.) cluster together in a highly supported group with individuals from Feijó, Reserva Extrativista (RE) Arapixi and Parque Ambiental (PA) Chico Mendes (Acre and Amazonas, Brazil) reported by Melo-Sampaio et al. (2018). This clade is retrieved with high support as sister to *A. aff. albiventris* SL5 from Ituxi River and Boca do Acre, which is followed by *A. aff. albiventris* SL3 from the Madeira River, *A. aff. albiventris* SL2 from the lower Juruá River and finally *A. aff. albiventris* SL1 from the middle Juruá River (Fig. 2).

Interspecific pairwise p distances within the *Allobates albiventris* species complex range from 1.2 to 4.8% (Table 1). The two smallest distances are between the new species (*Allobates albiventris* sp. nov.) and *A. aff. albiventris* SL3 (1.9%; 1.6–2.1%) and between the new species and *A. aff. albiventris* SL5 (2.0%; 1.2–2.4%). Although samples of the new species are widely distributed across the Brazilian State of Acre, genetic p distances between newly sequenced individuals of the new species and those reported by Melo-Sampaio et al. (2018) are very low (0.2%; 0.0–0.4%). The small genotypic divergence is congruent with low levels of phenotypic and bioacoustic divergence observed within the new species (see below).

Single-locus DNA delimitation

The best-ranked partition computed by ASAP (score = 3.5; $p = 0.001$; $w = 0.0006$) delimits all five clades within the species complex as distinct species (Fig. 2). The best ASAP threshold distance for the 16S dataset in this partition is 1%. As expected, the delimitation resulting from ABGD resembles that of ASAP and delimits the same five species (Fig. 2). On the other hand, GMYC is less conservative and delimits seven species by splitting the new species and *A. aff. albiventris* SL5 into two species each (Fig. 2). The majority rule consensus of these single-locus delimitation methods supports the delimitation of five species in the *Allobates albiventris* species complex.

Table 2. Loadings of morphometric variables on the first two shape principal components (PC) based on 28 male and 22 female *Allobates gasconi* sensu stricto and *Allobates albiventris* sp. nov. Numbers in bold denote variables that make the highest contributions to each shape PC. Measurement acronyms are described in the text; n, sample size.

Variables	Males		Females	
	shape.PC1	shape.PC2	shape.PC1	shape.PC2
DPT	−0.047	−0.203	−0.088	−0.067
EL	−0.043	0.029	0.048	0.071
EN	0.415	−0.008	0.335	−0.026
FAL	0.073	0.037	0.047	0.171
FL	0.137	0.147	0.115	0.071
HANDI	0.037	0.056	0.083	0.158
HANDII	0.02	0.11	0.051	0.118
HANDIII	0.082	0.037	0.052	0.075
HANDIV	0.038	0.103	0.06	0.091
HL	−0.197	0.112	−0.172	0.104
HW	−0.135	0.133	−0.161	0.126
IN	0.082	0.007	0.032	0.07
IO	−0.026	0.101	−0.029	0.097
SL	0.406	0.088	0.345	0.051
SVL	0.044	0.026	0.039	0.054
THL	0.03	0.142	0.016	0.083
TIL	0.035	0.204	0.014	0.072
TYM	−0.161	−0.07	−0.081	−0.04
UAL	0.002	0.118	0.003	0.015
WFD	−0.231	0.033	−0.154	−0.123
WPF	−0.617	−0.213	−0.775	−0.158
WTD	−0.187	−0.147	0.029	−0.124
WTT	0.247	−0.843	0.191	−0.887

Morphological analyses

The first two principal components of the Shape PCA performed with 23 morphometric measurements of *A. gasconi* sensu stricto and the new species together explain 64.6% and 63.1% of the variance of males and females, respectively (Table 2). Although the two respective shape spaces do not overlap in graphical representations of shape PC1 against PC2 (Fig. 3A, C), body shape is statistically different only in shape PC1 (ANOVAs: male, $S^2 = 2.7$, $F = 221.5$, $df = 44$, $p < .0001$; female, $S^2 = 2.2$, $F = 142.2$, $df = 22$, $p < .0001$). Width of finger III (WPF),

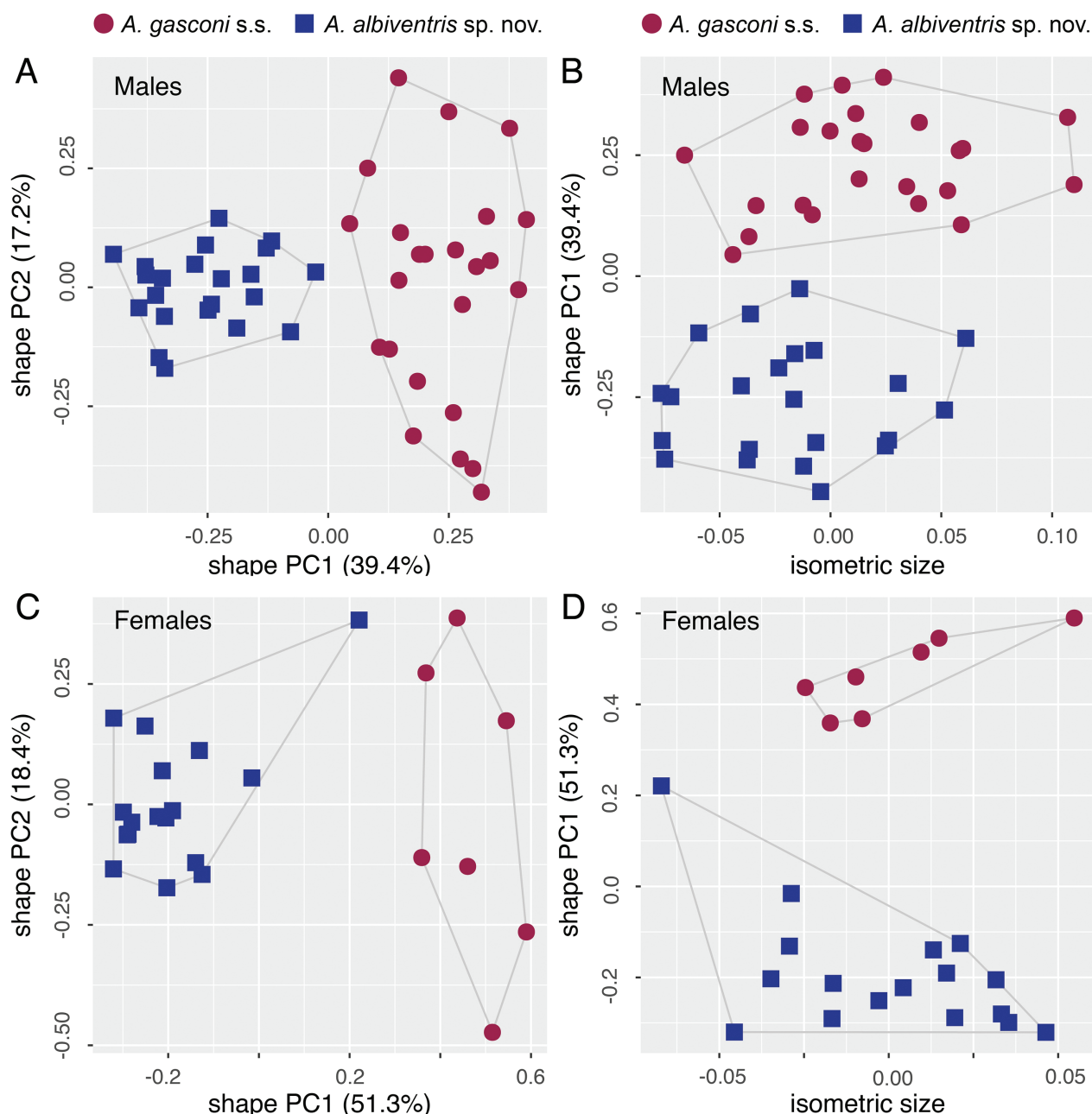


Figure 3. Shape Principal Component Analysis and isometric size of *Allobates gasconi* sensu stricto and *A. albiventris* sp. nov. Analyses are based on 23 morphometric measurements of 28 males (A, B) and 22 females (C, D). Abbreviation: s.s., sensu stricto.

eye–nostril distance (EN) and snout length (SL) strongly contribute to the variation of shape PC1 of both males and females (Table 2). The new species and *A. gasconi* sensu stricto also differ in the isometric size of males (ANOVA: $S^2 = 0.01$, $F = 8.3$, $df = 44$, $p = 0.006$), with the new species being larger (Fig. 3B).

Taxonomy

Allobates albiventris sp. nov.

<https://zoobank.org/DA65FF02-5C2B-4BF9-BDAF-B460B7A5A13E>

Chresonymy. *Allobates gasconi* – Melo-Sampaio et al. (2018), Lima et al. (2020), Gagliardi-Urrutia et al. (2021), Jaramillo et al. (2021), Silva et al. (2022). *Allobates gasconi* C – Souza et al. (2020). *Allobates gasconi* SL4 – Ferreira et al. (2023).

Holotype. INPAH45035 (field number APL21526), an adult male collected by J.R.D. Souza on February 5, 2020, in a forest fragment near BR 364 (08°52'27"S, 69°17'07"W, 166 m asl), municipality of Manoel Urbano, State of Acre, Brazil.

Paratopotypes. Nineteen adult specimens collected by J.R.D. Souza and A.P. Lima at the same locality as the holotype: 13 males INPAH45036–40 (field numbers APL21371–75), INPAH45042–47 (field numbers 21479–

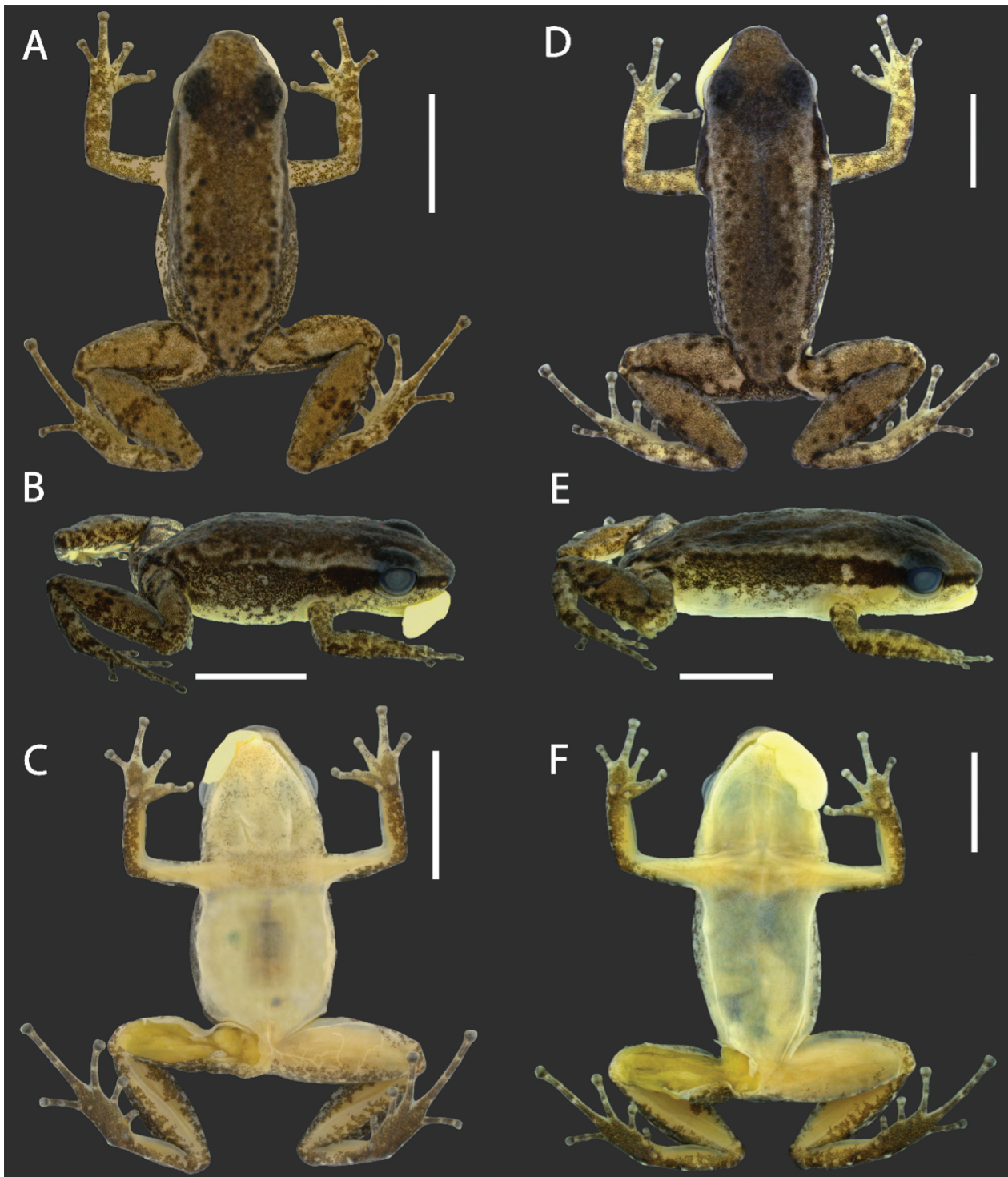


Figure 4. Dorsal, dorsolateral and ventral views of the male holotype INPAH45035 (A–C) and a female paratype INPAH45051 (D–F) of *Allobates albiventris* **sp. nov.** Scale bar: 5 mm. Photographs by J.R.D. Souza.

80, 21511, 21518, 21525 and 21528, respectively) and MPEG44609–10 (field numbers APL21370 and 21380, respectively), and six females INPAH45048–51 (field numbers APL21476, 21481, 21512 and 21527, respectively) and MPEG44611–12 (field numbers APL21478 and 21515, respectively).

Paratypes. Twenty-three adult specimens collected between 2018 and 2020 by J.R.D. Souza in the State of Acre, and between 2015 and 2016 by P.R. Melo-Sam-

paio in the States of Acre and Amazonas. ACRE: 10 females MPEG44607 (field number APL21355), INPAH45052–59 (field numbers APL21357, 21523–24 and 21530–34, respectively) and MPEG44613 (field number APL21522) and 7 males INPAH45060–63 (field numbers APL21520–21, 21354 and 21356, respectively), MPEG44608 (field number APL21358), MPEG44606 (field number APL21352) and MNRJ91679 (GenBank KY886578) from Parque Ambiental Chico Mendes (10°02'13"S, 67°47'36"W, 158 m asl), municipality of

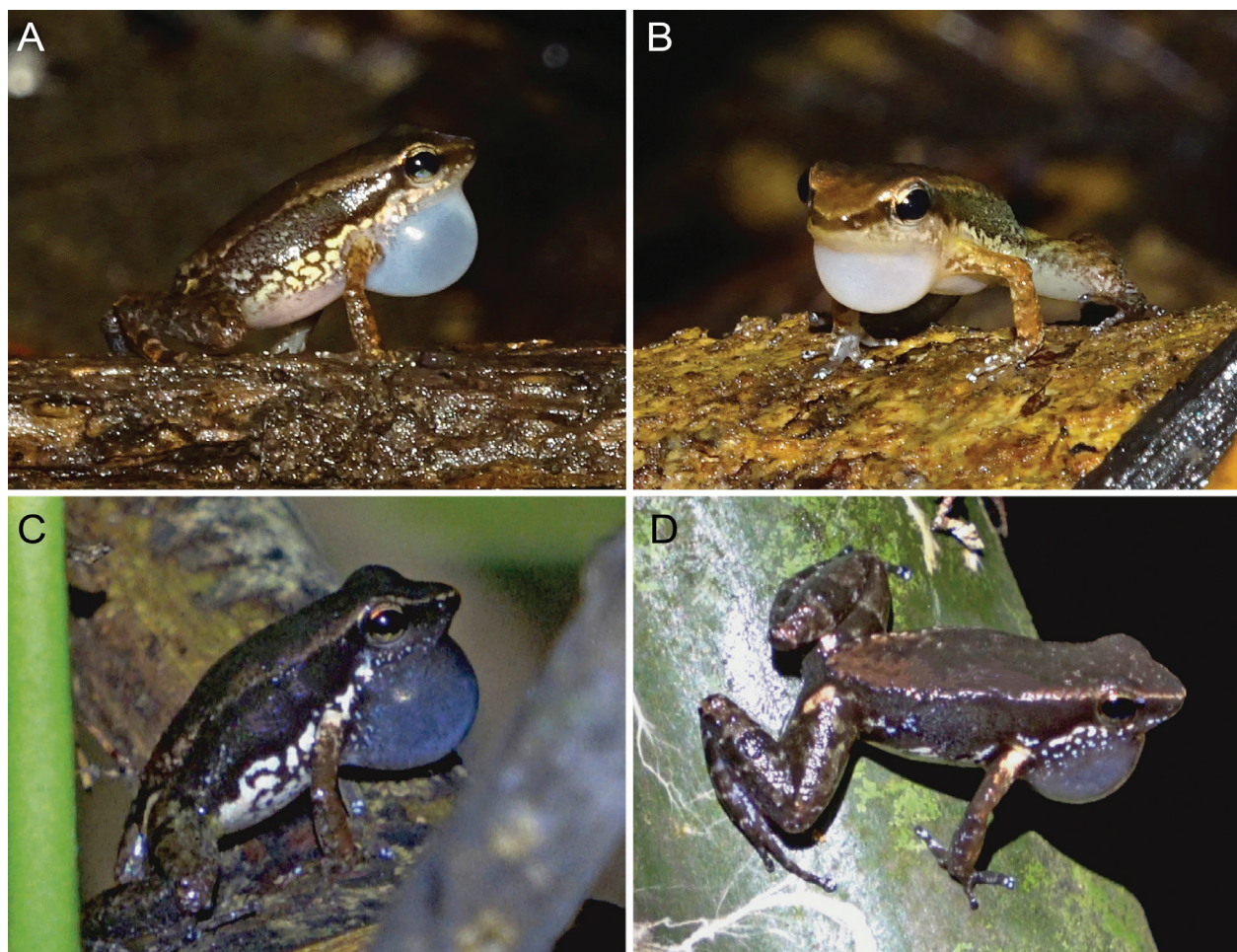


Figure 5. Coloration of the vocal sac and throat of *Allobates albiventris* sp. nov. (A, B) and *A. gasconi* sensu stricto (C, D). Photographs by J.R.D. Souza (A, B) and A.P. Lima (C, D).

Rio Branco; and 2 males INPAH45064–65 (field numbers APL21350–51, respectively) collected near the bank of the Antimary River (09°29'16"S, 68°21'20"W, 168 m asl.); one female MNRJ91665 (GenBank KY886576) and one male MCP13630 (GenBank KY886577) from the municipality of Feijó (08°14'13"S, 70°22'44"W, 184 m asl). AMAZONAS: one male MNRJ91683 (GenBank KY886574) and one female MNRJ91684 (GenBank KY886575) from Reserva Extrativista Arapixi (08°58'21"S, 67°51'50"W, 125 m asl), municipality of Boca do Acre.

Referred specimen. Brazil: Acre, one male (PRMS0360) collected by P.R. Melo-Sampaio on January 25, 2016, in Reserva Extrativista Arapixi, municipality of Boca do Acre.

Etymology. The specific epithet *albiventris* is a combination of two Latin words, *albus* (white) and *ventris* (venter), in reference to the pale ventral coloration of the new species. Vernacular names: pale-ventered nurse frog (English), rana cuidadora de vientre blanco (Spanish), and rãzinha cuidadora de ventre branco (Portuguese).

Generic placement. The new species is allocated to the genus *Allobates* based on molecular phylogenetic anal-

ysis and phenotypic characters proposed by Grant et al. (2017): paired dorsal digital scutes (character 2), tip of finger IV reaches the distal half of distal subarticular tubercle of finger III (character 5), finger III swollen in adult males (character 21), toe IV with basal webbing and lateral fringe on its preaxial side (characters 43), pale paracloacal marks (character 50) and absence of median lingual process (character 85).

Definition. *Allobates albiventris* sp. nov. is characterized by small adult size, SVL 14.3–16.4 mm ($n = 22$) in males and 15.6–17.8 mm ($n = 16$) in females. Dorsum smooth with a high concentration of granules in the medium posterior portion. Snout semi-truncated and semi-acuminate in dorsal and lateral views; *canthus rostralis* almost straight in dorsal view; loreal region flat; nostrils visible in ventral and lateral views. Tympanum diameter 34–48% of EL. Maxillary teeth present, visible under magnification; median lingual process absent. One subarticular tubercle on finger IV; fingers II and III weakly swollen in adult males; disc on finger II approximately the same width as distal phalanx; width of discs on fingers I, III and IV represent 1.3 ± 0.3 , 1.5 ± 0.2 and 1.6 ± 0.2 of width of respective distal phalanges; tip of finger IV reaches the distal subarticular tubercle of finger III; nuptial excrescence on thumb absent; lateral keels present on fingers

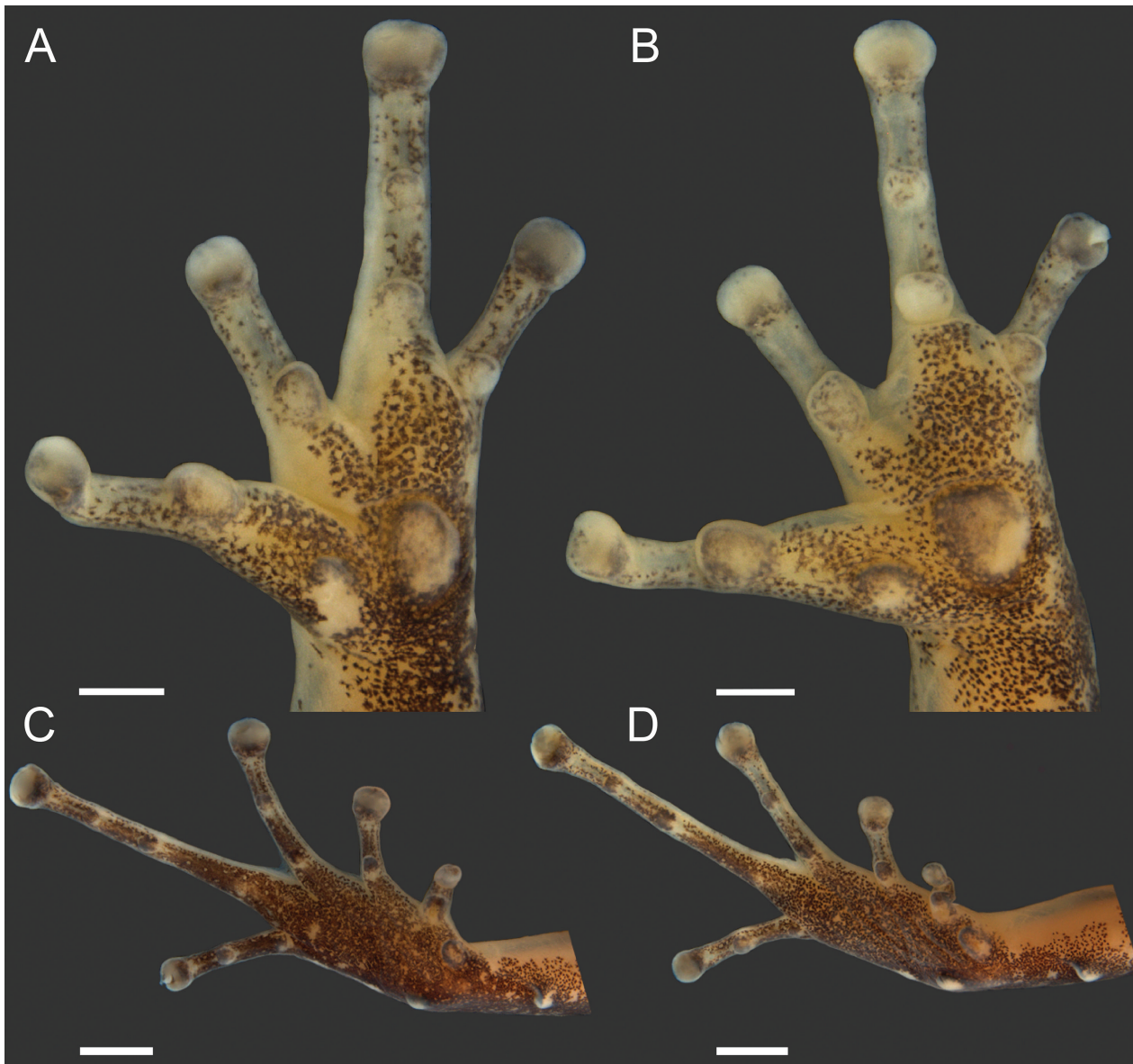


Figure 6. Ventral view of the hand (A, B) and foot (C, D) of *Allobates albiventris* sp. nov. (A, C) Male holotype INPAH45035. (B, D) Female paratype INPAH45051. Scale bar: 0.5 mm (A, B) and 1 mm (C, D). Photographs by J.R.D. Souza.

II–IV; supernumerary tubercles and metacarpal ridge absent; webbing absent between fingers; black gland absent on arm; tarsal keel present, tubercle-like, strongly curved towards the inner metatarsal tubercle; basal webbing present between toes II–IV, less developed between toes II and III; discs on toes II–V moderately expanded; disc on toe I not expanded, approximately the same width of distal phalanx; lateral keels present on all toes. Dorsum light brown with a dark brown band, diamond or hourglass-shaped marks; pale dorsolateral stripe present in preserved specimens, with an irregular upper border extending from the posterior region of the eyelids to the posteromedial region of the body or urostyle; pale ventrolateral stripe absent in preservative, discontinued when present in living specimens; dark brown oblique lateral stripe present, narrower from snout to anterior corner of eye, wider from the posterior corner of the eye to the groin, with an irregular lower border. Paired dorsal digital scutes white. Cream-colored forelimbs with scattered

dark brown spots and blotches. Hind limbs light brown; anterior and dorsal portions of the thigh with dark brown spots, dorsal region light brown with scattered spots; a dark brown transverse bar present on thigh of some individuals, usually on tibia; comma-shaped, light brown to orange paracloacal mark. In life, males and females have a white belly and chest without melanophores; throat and vocal sac of males translucent white with scattered melanophores; throat white centrally and posteriorly, translucent laterally and anteriorly in females, with scattered melanophores distributed in the anterior region of the maxilla. Unpigmented intestine. Dark brown mature oocyte; unpigmented testes. Advertisement call with a duration of 42–60 ms and comprising two notes (the first note is shorter than the second), with an inter-note interval of 8–23 ms and dominant frequency of 4,953–6,331 Hz. Exotrophic tadpoles with 2 pyramidal papillae on each end of the anterior labium; 10–13 pyramidal and cylindrical papillae on the posterior labium; LTRF = 2(2)/3(1); gap

in row A-2 \approx 40% of A-1; relative length P-1 > P-2 > P-3; and P-3 \approx 65% of P-1.

Diagnosis. *Allobates albiventris* sp. nov. differs from other *Allobates* by the following combination of characters: males in life with a throat and vocal sac translucent white with melanophores uniformly distributed and a white belly; females in life with throat white centrally and posteriorly, translucent laterally and anteriorly, chest and belly white; small adult size, SVL 14.3–16.4 mm ($n = 22$) in males and 15.6–17.8 mm ($n = 16$) in females; one subarticular tubercle on finger IV; finger III of adult males weakly swollen; disc of finger II approximately the same width as the distal phalanx; interdigital membranes present between toes II, III and IV; paired digital scutes white; advertisement call with a duration of 42–60 ms and comprising two notes (the first note is smaller than the second), with an inter-note interval of 8–23 ms and dominant frequency of 4,953–6,331 Hz; exotrophic tadpoles with 2 pyramidal papillae on each end of the anterior labium, 10–13 pyramidal and cylindrical papillae on the posterior labium, LTRF = 2(2)/3(1), gap in row A-2 \approx 40% of A-1, relative length P-1 > P-2 > P-3, and P-3 \approx 65% of P-1.

Comparisons. Characteristics of the compared species are presented within parentheses unless stated otherwise. Males of *Allobates albiventris* sp. nov. are easily distinguished from those of *A. flaviventris*, *A. fuscellus*, *A. grillicantus*, *A. kamilae*, *A. melanolaemus*, *A. nidicola*, *A. ornatus*, *A. paleci*, *A. paleovarzensis*, *A. tapajos*, *A. tinae*, *A. trilineatus*, *A. vanzolinus* and *A. velocicantus* by having a translucent white throat and vocal sac in life (violaceous to gray in *A. flaviventris*, *A. pacaas* and *A. paleovarzensis*; yellow in *A. grillicantus*, *A. kamilae*, *A. paleci*, *A. tapajos* and *A. tinae*; gray to black in *A. fuscellus*, *A. melanolaemus*, *A. nidicola*, *A. trilineatus* and *A. vanzolinus*; gray in *A. ornatus*; whitish centrally and yellow laterally in *A. velocicantus*). Additionally, *A. albiventris* sp. nov. differs from *A. pacaas* by having only one subarticular tubercle on finger IV (two tubercles); from *A. tapajos* by the presence of melanophores on the vocal sac of males (absent); from *A. flaviventris*, *A. nidicola*, *A. paleovarzensis* and *A. vanzolinus* by having a maximum SVL of 16.4 mm in males (minimum SVL 16.7 mm in *A. flaviventris*, 18.5 mm in *A. nidicola*, 18.3 mm in *A. paleovarzensis* and 21.5 mm in *A. vanzolinus*).

Males of *Allobates caeruleodactylus*, *A. conspicuus*, *A. grillisimilis*, *A. subfolionidificans* and *A. sieggreenae* have a throat and vocal sac coloration similar to *A. albiventris* sp. nov. However, *A. albiventris* sp. nov. differs from these species by the presence of dark marks or a dark brown, wide longitudinal band on the dorsum (uniform light brown dorsum in all mentioned species). In addition, *A. albiventris* sp. nov. differs from *A. caeruleodactylus* by having white digital scutes in life (blue); from *A. conspicuus* and *A. sieggreenae* by the absence of a continuous ventrolateral stripe (ventrolateral stripe present); from *A. grillisimilis* by having regularly distributed melanophores on the throat, vocal sac and chest

(melanophores, when present, only on the jaw); and from *A. subfolionidificans* by having a dorsolateral stripe (absent) and females in life with a white chest and belly (yellow).

Although *A. albiventris* sp. nov. has been confused with *A. gasconi*, they are easily distinguished by the coloration of breeding adults. Males of the new species are easily distinguished from those of *A. gasconi* sensu stricto by the translucent white throat and vocal sac (gray to dark gray; Fig. 5), white chest (translucent to pinkish grey) and white belly without melanophores (belly pinkish grey anteriorly, whitish grey centrally, light or translucent grey with white and brown small blotches laterally, and yellowish or translucent grey posteriorly; Ferreira et al. 2023; present study). Female *A. albiventris* sp. nov. have a white throat centrally and posteriorly but translucent laterally and anteriorly (light to bright yellow), a white chest (bright to whitish yellow) and a white belly (belly yellowish to whitish cream). Moreover, finger III of adult males is only slightly swollen (moderately to highly swollen; Ferreira et al. 2023; present study).

The advertisement calls of *Allobates albiventris* sp. nov. differ from *A. gasconi* sensu stricto by a call duration of 50 ± 4 ms (94 ± 33 ms), exclusively composed of 2 notes (2–4 notes, mainly 3 notes) with the first note always shorter than the second (notes with similar duration) and an inter-note interval of 16 ± 4 ms (30 ± 4 ms; Ferreira et al. 2023). Calls of *A. albiventris* sp. nov. and *A. trilineatus* are similar: both are composed of two notes and are arranged in call series. However, the former species differs from *A. trilineatus* by having a call duration of 42–60 ms (60–80 ms) and the first note always shorter and with a lower dominant frequency than the second one (similar duration and dominant frequency in both notes; Jaramillo et al. 2021). Calls of *A. albiventris* sp. nov. have two notes exclusively, which differs from *A. caeruleodactylus*, *A. melanolaemus*, *A. nidicola*, *A. paleovarzensis*, *A. sieggreenae*, *A. subfolionidificans*, *A. tapajos* and *A. tinae* (calls composed of one note in each species). Moreover, calls of *A. albiventris* sp. nov. are commonly arranged in call series (single calls emitted regularly through time in *A. caeruleodactylus*, *A. nidicola* and *A. subfolionidificans*) with a call duration of 42–60 ms (151–507 ms in *A. grillicantus*; 122–305 ms in *A. grillisimilis*; 180–340 ms in *A. paleci*; and 1,870–2,890 ms in *A. velocicantus*) and are composed exclusively of two notes (3–15 notes in *A. grillicantus* and *A. grillisimilis*; 16–33 ms in *A. paleci*; and 66–138 in *A. velocicantus*). As in *A. albiventris* sp. nov., regular calls of *A. flaviventris* are composed of two notes, but in the former species calls are emitted with a dominant frequency of 4,953–6,331 Hz (3,618–4,651 Hz in *A. flaviventris*). The advertisement calls of *A. conspicuus*, *A. fuscellus*, *A. ornatus*, *A. pacaas* and *A. vanzolinus* are unknown.

Tadpoles of *Allobates albiventris* sp. nov. easily differ from those of *A. gasconi* sensu stricto by having a LTRF = 2(2)/3(1) and a tail highly pigmented with brown spots of various shapes and sizes resembling a marbled pattern (LTRF = 2(2)/2(1) and a tail poorly pigmented with brown spots; Ferreira et al. 2023); from those of *A.*

Table 3. Morphometric measurements in millimeters of *Allobates albiventris* sp. nov. and *A. gasconi* sensu stricto. Values represent mean ± standard deviation (range). Measurement acronyms are described in the text; n, sample size.

Characters	<i>Allobates albiventris</i> sp. nov.			<i>Allobates gasconi</i> sensu stricto	
	Holotype	Males (n = 21)	Females (n = 16)	Males (n = 24)	Females (n = 7)
SVL	14.6	15.3±0.5 (14.3–16.4)	16.5±0.5 (15.6–17.8)	16.2±0.6 (14.8–17.1)	16.8±0.8 (16.0–18.0)
IOD	4.5	4.6±0.2 (4.3–5.0)	4.8±0.2 (4.5–5.1)	4.7±0.3 (4.3–5.5)	4.7±0.2 (4.3–4.9)
HW	5.1	5.1±0.2 (4.8–5.5)	5.5±0.2 (5.1–5.9)	4.9±0.3 (4.3–6.0)	4.9±0.2 (4.5–5.1)
HL	4.9	4.9±0.2 (4.6–5.4)	5.3±0.2 (4.9–5.8)	4.6±0.4 (4.0–5.7)	4.7±0.3 (4.3–4.9)
IND	2.2	2.2±0.1 (2.0–2.5)	2.4±0.1 (2.3–2.6)	2.4±0.1 (2.2–2.7)	2.5±0.1 (2.3–2.6)
THL	7.0	7.0±0.4 (6.4–8.0)	7.3±0.2 (7.0–7.9)	7.4±0.6 (6.5–8.8)	7.4±0.3 (7.0–7.8)
TIL	7.1	7.3±0.4 (6.7–8.1)	7.6±0.2 (7.4–8.0)	7.7±0.6 (6.6–9.2)	7.7±0.4 (7.2–8.1)
FL	6.9	6.7±0.4 (6.1–7.7)	6.9±0.3 (6.6–7.3)	7.4±0.5 (6.6–8.9)	7.5±0.3 (7.0–8.1)
UAL	3.6	3.8±0.2 (3.5–4.2)	4.0±0.2 (3.6–4.3)	4.0±0.2 (3.5–4.5)	3.9±0.2 (3.8–4.4)
FAL	3.3	3.4±0.2 (3.1–3.8)	3.6±0.5 (3.3–5.6)	3.6±0.3 (2.9–4.4)	3.7±0.3 (3.5–4.3)
HANDI	2.6	2.7±0.1 (2.5–2.9)	2.8±0.1 (2.6–3.0)	2.9±0.2 (2.4–3.3)	3.0±0.2 (2.8–3.2)
HANDII	2.5	2.6±0.1 (2.4–2.8)	2.7±0.1 (2.5–2.9)	2.7±0.2 (2.4–3.1)	2.8±0.1 (2.6–3.0)
HANDIII	3.5	3.6±0.2 (3.2–4.0)	3.8±0.1 (3.5–4.1)	3.9±0.3 (3.4–4.4)	4.0±0.2 (3.8–4.2)
HANDIV	2.3	2.4±0.2 (2.1–2.7)	2.5±0.1 (2.4–2.7)	2.6±0.3 (2.0–3.1)	2.7±0.1 (2.5–2.8)
WFD	0.5	0.5±0.1 (0.4–0.6)	0.6±0.0 (0.5–0.7)	0.5±0.1 (0.4–0.6)	0.5±0.0 (0.5–0.6)
WPF	0.3	0.3±0.0 (0.2–0.4)	0.3±0.0 (0.3–0.4)	0.4±0.1 (0.3–0.5)	0.3±0.0 (0.3–0.4)
DPT	0.5	0.5±0.1 (0.5–0.6)	0.6±0.0 (0.5–0.7)	0.6±0.1 (0.4–0.8)	0.5±0.0 (0.5–0.6)
WTT	0.4	0.4±0.0 (0.3–0.4)	0.4±0.0 (0.3–0.5)	0.5±0.1 (0.3–0.7)	0.5±0.1 (0.3–0.7)
WTD	0.6	0.7±0.1 (0.5–0.8)	0.7±0.1 (0.6–0.8)	0.6±0.1 (0.5–0.7)	0.7±0.1 (0.6–0.8)
TYM	0.8	0.9±0.1 (0.7–1.1)	0.9±0.1 (0.9–1.1)	0.8±0.1 (0.6–0.9)	0.9±0.1 (0.6–0.9)
EL	2.0	2.1±0.1 (2.0–2.4)	2.2±0.1 (2.1–2.4)	2.1±0.1 (1.9–2.4)	2.3±0.1 (2.1–2.5)
END	1.5	1.4±0.1 (1.2–1.8)	1.5±0.1 (1.4–1.7)	1.9±0.2 (1.4–2.1)	1.9±0.1 (1.8–2.0)
SL	2.2	2.0±0.2 (1.7–2.4)	2.1±0.1 (1.9–2.4)	2.5±0.2 (2.1–2.9)	2.7±0.1 (2.5–2.8)

nicicola by being exotrophic and having a spiracle (endotrophic, spiracle absent); from *A. subfolionidificans* and *A. tapajos* by having two pyramidal papillae on each side of the anterior labium (six in *A. subfolionidificans*; four or five in *A. tapajos*); from *A. velocicantus* by having pyramidal and cylindrical papillae on the posterior labium (only pyramidal in *A. velocicantus*); from *A. grillicantus* by having LTRF = 2(2)/3(1) [LTRF = 2(2)/3 in *A. grillicantus*]; from *A. grillisimilis* and *A. paleovarzensis* by having LTRF = P-1 > P-2 > P-3 (P-3 = P-2 = P-1 in *A. grillisimilis*; P-2 > P-1 > P-3 in *A. paleovarzensis*); from *A. caeruleodactylus* by the gap in row A-2 ≈ 40% of A-1 and P-3 ≈ 65% of P-1 (A-2 gap ≈ 58% of A-1 and P-3 ≈ 37% of P-1 in *A. caeruleodactylus*). Tadpoles of *A. conspicuus*, *A. flaviventris*, *A. fuscillus*, *A. melanolaemus*, *A. ornatus*, *A. pacaas*, *A. tinae*, *A. sieggreenae*, *A. trilineatus* and *A. vanzolinius* are unknown.

Description of the holotype. Adult male, INPAH45035 (Figs 4A–C; 6A, C; 8A–C; Table 3). Snout-vent length 14.6 mm. Head wider than long (HW/HL = 1.04); HW equals 35% of SVL and HL equals 33% of SVL. Eye diameter exceeds distance from eye to nostril (EL/END = 1.33); EL equals 43% of HL. Interorbital region flat; IOD equals 88% of HW. Tympanum rounded, visible to the naked eye. Snout slightly rounded in dorsal and lateral view. Inter-nostril region flat; nostrils rounded, laterally positioned and visible in lateral and ventral view; IND equals 49% of IOD. *Canthus rostralis* straight in dorsal view; loreal region flat. Maxillary teeth present. Median

lingual process absent. Vocal sac single, subgular. Lateral folds of vocal sac present at the level of angle of maxilla.

Palmar tubercle rounded and conspicuous, diameter 0.42 mm. Thenar tubercle elliptical and conspicuous, width 0.29 mm. Diameter of thenar tubercle equals 69% of that of the palmar tubercle. Subarticular tubercles protruding, oval on finger I and rounded in other fingers; two tubercles on finger III but one in each of the others; distal tubercle smaller than proximal tubercle on finger III; tubercle on finger I larger than others. Supernumerary tubercles absent. Lateral keels on fingers I–IV, poorly defined on finger I. When placed side by side, the tip of finger IV reaches the distal subarticular tubercle of finger III. Preaxial phalangeal swelling on finger II and III. Relative length of fingers: IV < II < I < III. Discs are wider than the third phalanx on fingers I, III and IV, but approximately the same width on finger II. Paired dorsal digital scutes present.

Tibia and thigh lengths approximately the same (TIL/THL = 1.01), equal 49% and 48% of SVL, respectively. Foot length 97% of tibia length. Tarsal keel conspicuous and curved, narrowing towards the internal metatarsal tubercle. Internal metatarsal tubercle protuberant, elliptical. External metatarsal tubercle small and round, protruding, smaller than diameter of internal metatarsal tubercle. Metatarsal fold absent. Lateral keels present on preaxial and postaxial sides of each toe. Basal webbing between toes II and IV. Subarticular tubercles rounded and evident; one each on toes I and II but two each on toes III–V.

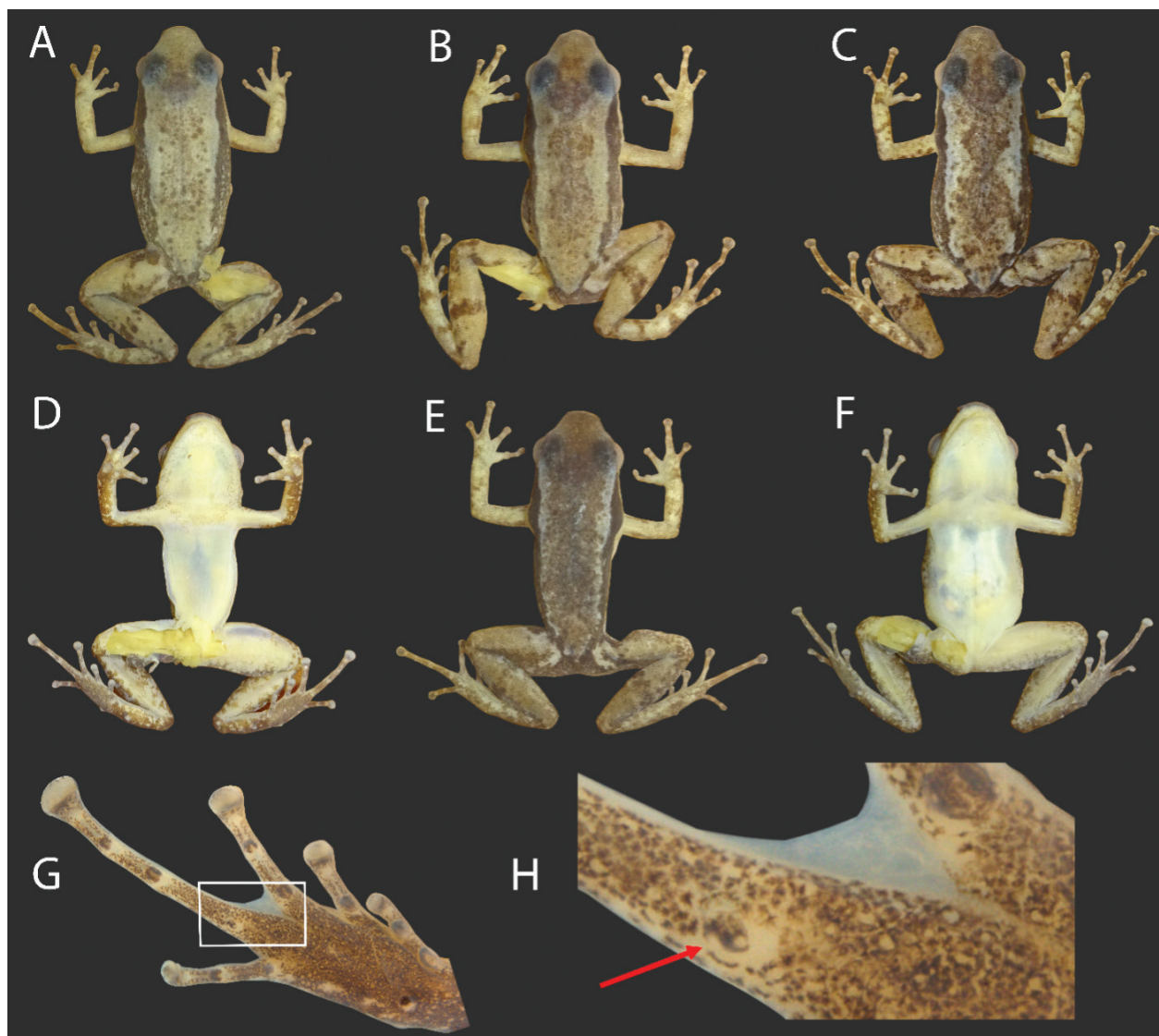


Figure 7. Paratypes of *Allobates albiventris* sp. nov. **A** Female, MPEG44612, SVL 16.2 mm. **B** Male, INPAH45038, SVL 14.7 mm. **C, F** Female, INPAH45054, SVL 17.0 mm. **D** Male, INPAH45060, SVL 15.6 mm. **E** Male, INPAH45046, SVL 14.9 mm. **G, H** Male, INPAH45064, SVL 16.4 mm. White rectangle in (**G**) delimits the magnified region (**H**) illustrating the third tubercle on toe IV (arrow). Photographs by J.R.D. Souza.

Discs rounded, wider than distal phalanx on toes II, III and IV but of similar width on toe I; disc of toe V with smaller expansion compared to toes II–IV. Paired dorsal digital scutes present.

Dorsal skin smooth with small flattened and barely visible tubercles, mostly on the posterior portion; skin on arms smooth; skin on legs smooth with small tubercles. Ventral surface of body, arms and legs smooth.

In preservative (Fig. 4A–C), dorsal surface of body and limbs light brown; numerous dark brown melanophores form a longitudinal band, which is slightly constrained behind the eyes and diffuse towards the cloaca (Fig. 4A). A narrow and cream-colored dorsolateral stripe with an irregular upper border extends from posterior region of eyelids to mid-posterior region of body (Fig. 4B). Lateral stripe dark brown; darkest from the tip of the snout to the region above the axilla; lower border regular on snout but irregular in ventrolateral region of body (Fig. 4B). Paler oblique stripe diffuse, extends from the

inguinal region to the axilla. Ventrolateral stripe absent. Ventrolateral region beige; melanophores form small dark brown irregular spots. Transverse dark brown bar on thigh and tibia is widest on tibia (Fig. 4A). Anterior region of thigh light brown, posterior region dark brown; paracloacal marks cream, conspicuous. Chest, throat and vocal sac cream with small dark brown melanophores; belly cream, lacks melanophores or dark spots. Ventral surface of arms beige with scarce brown melanophores; light brown on forearms. Mid-ventral surface of thigh and tibia cream, without melanophores; ventrolateral surface with irregular dark brown spots (Fig. 4C). Palmar and plantar surfaces dark brown (Figs 4C, 5A, C). Tongue longer than wide, with anterior third attached to the floor of the mouth, cream-colored (Fig. 4B).

Coloration in life is similar to that in preservative. Dark marks, spots, stripes, lines and bars are more conspicuous. Background coloration of the dorsum cream. Ventrolateral stripe discontinuous from the posterior



Figure 8. Coloration in life of *Allobates albiventris* sp. nov. from Manoel Urbano and Rio Branco, State of Acre, Brazil. **A–C** Male holotype, SVL 14.6 mm; **D–F** Female, INPAH45051, SVL 16.8 mm; **G–I** Male, MNRJ 91679, SVL 16.0 mm; **J–L** Female, MPEG44613, SVL 16.0 mm; **M** Male, uncollected; **N** Male, INPAH45044, SVL 15.3 mm; **O** Male, uncollected. Photographs by J.R.D. Souza (A–F, J–O) and P.R. Melo-Sampaio (G–I).

corner of the eye to the axilla; small iridescent dots and spots visible below the dark brown band (Fig. 8A–C). Iris metallic bronze, pupil black. Ventral surface of arms and

legs varies between light gray and rosaceous gray. Throat and vocal sac translucent white; chest and belly white. Paired digital dorsal scutes white.

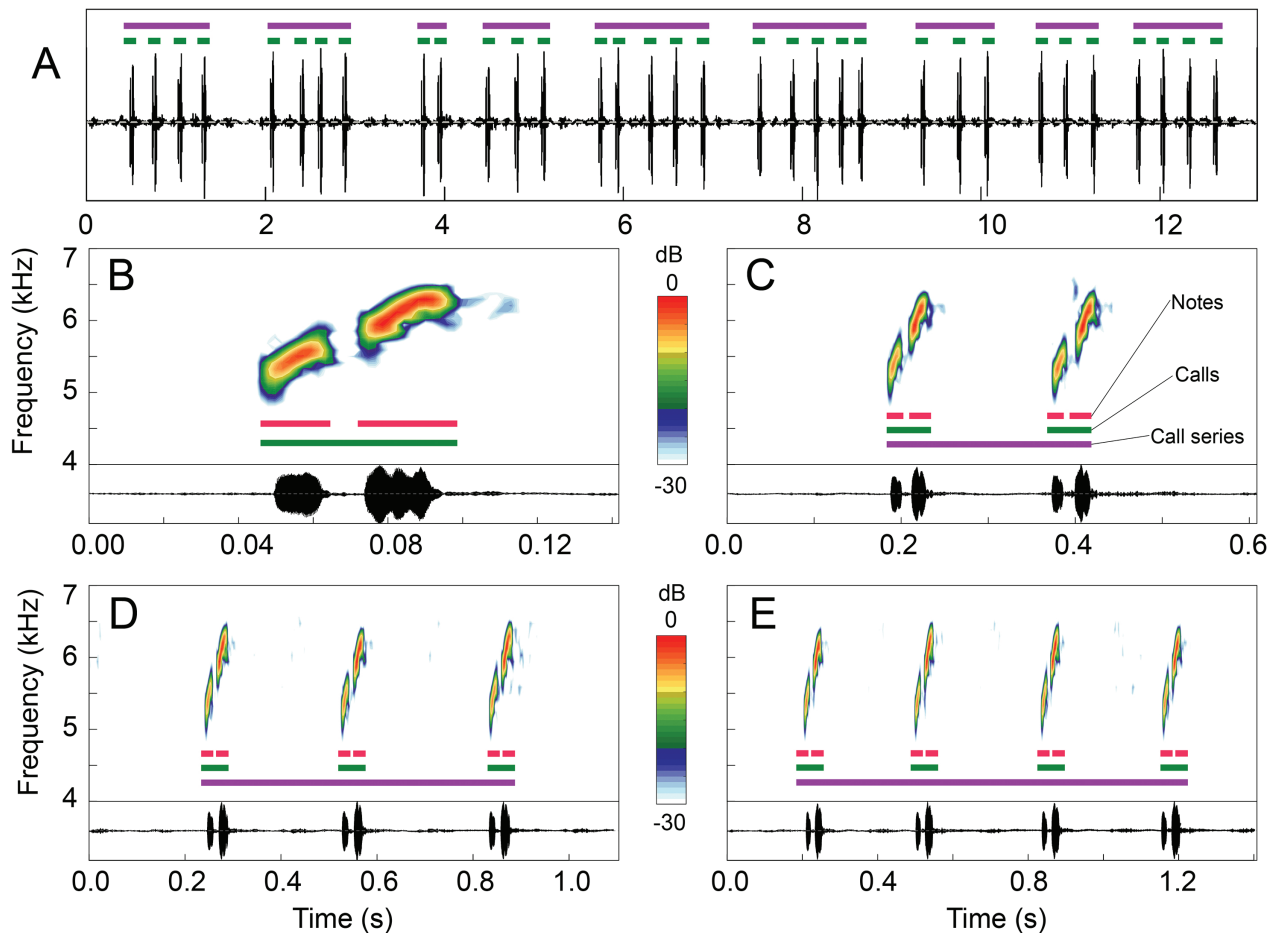


Figure 9. Advertisement calls of the holotype of *Allobates albiventris* sp. nov. (INPAH45035, FJNV 53687). **A** Oscillogram showing the continuous emission of calls with variable arrangements. Spectrograms and oscillograms of the four most common call arrangements: single call (**B**) and series of two (**C**), three (**D**) and four calls (**D**). Note that each call is composed of two notes. Air temperature: 22°C. Abbreviations: dB, decibels; kHz, kilohertz; s, seconds.

Variation in the type series. Variation in morphometric measurements of *Allobates albiventris* sp. nov. is summarized in Table 3. Sexual dimorphism is present in SVL and 12 body ratios. Females are larger than males (SVL; $S^2 = 10.3$, $F = 50.48$, $df = 36$, $adj\ p = 0.0002$) but smaller in EN ($S^2 = 0.0006$, $F = 8.46$, $df = 33$, $adj\ p = 0.0152$), THL ($S^2 = 0.0028$, $F = 20.94$, $df = 33$, $adj\ p = 0.0004$), TIL ($S^2 = 0.0073$, $F = 11.64$, $df = 36$, $adj\ p = 0.0062$), FL ($S^2 = 0.0025$, $F = 8.31$, $df = 36$, $adj\ p = 0.0152$), UAL ($S^2 = 0.0010$, $F = 7.55$, $df = 36$, $adj\ p = 0.0195$), FAL ($S^2 = 0.0006$, $F = 6.58$, $df = 33$, $adj\ p = 0.0266$), HANDI ($S^2 = 0.0005$, $F = 8.87$, $df = 36$, $adj\ p = 0.0148$), HANDII ($S^2 = 0.0004$, $F = 9.33$, $df = 36$, $adj\ p = 0.0139$), HANDIV ($S^2 = 0.0005$, $F = 7.09$, $df = 36$, $adj\ p = 0.0220$), WPF ($S^2 = 0.00003$, $F = 42.28$, $df = 27$, $adj\ p < .0001$), WTT ($S^2 = 0.00002$, $F = 38.79$, $df = 27$, $adj\ p < .0001$) and EL ($S^2 = 0.0003$, $F = 13.55$, $df = 36$, $adj\ p = 0.0035$).

Unlike the holotype, a third subarticular tubercle is present on the proximal portion of toe IV in 53% of the rest of the type series (12 males and 8 females). When present, it is approximately half the size of other subarticular tubercles on the same toe (Fig. 7G, H).

In preservative, dorsal coloration of the type series ranges from light to dark brown (Fig. 7). Dark hour-glass-like markings are present in 45% of males ($n = 10$)

and 44% of females ($n = 7$) and are more noticeable in individuals with lighter background coloration (e.g., Fig. 7B, C). In the other specimens, a light-to-dark-brown band extends down the center of the dorsum from the interorbital region to the urostyle. The light dorsolateral line is present in all males and females. However, its variable thickness is more evident in specimens lacking hour-glass markings (Fig. 7E). Conspicuous dark transverse bars on the tibia, which are barely visible or absent on the thigh, are present in 71% of specimens (12 males and 15 females). Both males and females lack visible melanophores on the belly (Fig. 7D, F) but the sexes differ with respect to the presence and concentration of melanophores on the chest and throat; melanophores are present on the chest in 72% of males ($n = 16$) but only 31% of females ($n = 5$). Although melanophores are present on the throat of all individuals, females have fewer of them and they are distributed mainly in the anterior and peripheral region of the throat, while males have more, evenly distributed, melanophores.

As in the holotype, coloration in life is similar to that in preservative (Fig. 7). The lateral brown stripe is darkest from the tip of the snout to the region above the axilla, becoming lighter and more diffuse as it extends to the inguinal region (Fig. 8A, E, H).

Table 4. Advertisement call parameters of *Allobates albiventris* sp. nov. Values represent the mean for each calling male. Call parameters are described in the text. Localities: ANT, Antimary River; FEI, Feijó; MUR, Manoel Urbano; PCM, Parque Ambiental Chico Mendes; REA, Reserva Extrativista Arapixi. Abbreviations: AT, air temperature in degrees Celsius; FNJV, call voucher recordings are deposited in the Fonoteca Neotropical Jacques Vielliard; SD, standard deviation.

FNJV	Locality	AT	CSD	ICSI	CD	ICI	ND1	INI	ND2	LFN1	HFN1	DFN1	LFN2	HFN2	DFN2
Unvouchered	FEI	NA	480	2,010	49	160	12	19	18	5,015	5,608	5,336	5,361	5,831	5,607
Unvouchered	PCM	NA	1,040	1,190	58	240	13	20	24	4,893	5,523	5,222	5,263	5,739	5,487
53688	PCM	23.0	1,560	1,210	52	210	11	21	20	5,448	6,048	5,792	5,875	6,336	6,141
53689	PCM	23.5	700	1,680	52	230	10	22	20	4,823	5,362	5,065	5,118	5,617	5,381
Unvouchered	REA	28.0	940	1,230	49	280	10	20	18	5,374	6,008	5,705	5,695	6,222	5,991
53692	REA	28.0	440	620	47	200	11	17	20	5,181	5,944	5,606	5,685	6,273	6,002
53693	REA	29.0	360	760	48	210	13	16	18	5,023	5,714	5,400	5,522	6,006	5,768
53680	ANT	25.0	790	920	48	210	12	16	20	4,739	5,213	5,017	5,276	5,658	5,476
53681	ANT	24.5	1,050	690	51	240	13	16	21	5,09	5,673	5,416	5,548	6,083	5,861
53682	MUR	24.0	670	640	49	230	15	14	19	5,194	5,621	5,405	5,619	6,070	5,840
53685	MUR	22.0	1,400	2,120	48	220	13	14	20	5,312	5,858	5,618	5,702	6,307	6,083
53686	MUR	22.0	650	730	45	200	13	11	21	5,352	5,941	5,591	5,995	6,507	6,294
53687	MUR	22.0	780	660	45	230	13	12	20	5,098	5,663	5,392	5,709	6,267	6,036
53684	MUR	22.0	630	880	47	200	16	11	20	5,179	5,73	5,465	5,702	6,176	5,978
53683	MUR	22.0	610	850	51	230	16	15	21	5,044	5,523	5,237	5,519	6,033	5,810
53691	MUR	22.0	440	560	45	160	13	12	21	5,084	5,638	5,353	5,568	6,082	5,825
53690	MUR	21.0	550	950	50	240	12	17	20	5,036	5,493	5,278	5,568	6,020	5,805
Mean	–	23.9	700	1,010	50	210	13	16	20	5,120	5,687	5,409	5,577	6,076	5,849
SD	–	2.6	650	670	4	50	2	4	2	206	228	211	233	247	250
Min	–	21.0	40	410	42	130	8	8	14	4,640	5,153	4,953	4,909	5,413	5,189
Max	–	29.0	4,470	4,400	60	390	20	23	26	5,576	6,127	5,857	6,195	6,552	6,331

Advertisement call. The advertisement call of *Allobates albiventris* sp. nov. is formed by a pair of notes that is emitted singly or in a series of as many as 16 calls. Calls emitted in series of one, two, three, four or five calls correspond to 88% of recorded call arrangements (Fig. 9A–E). Calls have an average duration of 50 ± 4 ms (42–60 ms). The first note of each call is always shorter (13 ± 2 ms; 8–20 ms) than the second one (20 ± 2 ms; 14–26 ms) (Fig. 10B), and the inter-note interval ranges from 8 to 23 ms (16 ± 4 ms). Call series with two calls have a duration of 220–610 ms (320 ± 70 ms), while series with three, four or five calls have a duration of 370–1,030 ms (600 ± 110 ms), 580–1,420 ms (950 ± 170 ms) and 790–1,700 ms ($1,260 \pm 200$ ms), respectively. The inter-call interval within call series is 130–390 ms (210 ± 50 ms); the interval between call series is 410–4,400 ms ($1,010 \pm 670$ ms). Notes have modulated frequencies, ascending from beginning to end (Fig. 10B–E). The first note has a slightly lower dominant frequency ($5,409 \pm 211$ Hz; 4,952–5,857 Hz) than the second note ($5,849 \pm 250$ Hz; 5,189–6,331 Hz). Lower and upper frequency values are presented in Table 4.

Eggs and larvae. Descriptions of quantitative characters of tadpoles are based on six specimens at Gosner stage 34. Morphometric measurements are presented in Table 5. Body ovoid in dorsal view, ellipsoid in lateral view (Fig. 10A–C). Body length (BL) 31–33% of total length (TL)

and tail length 67–69% of TL; body wider than tall (BH 50–65% of BW) and longer than wide (BW 61–80% of BL); HWLE 72–93% of BW; snout rounded in dorsal and lateral view; END 60–78% of ED; eyes directed dorsally and laterally; IOD 26–33% of HWLE. Nostrils located dorsolaterally and directed anterolaterally, visible in dorsal and lateral view; inter-nostril distance 38–44% of HWLE. Fleshy ring present on inner margin of nostrils, round, not ornamented. Spiracle single, sinistral, tubular, 0.46–0.67 mm long; it is attached laterally, a little below half body length and just dorsal to the intestine. Gut coiled. Vent tube dextral, 1.23–1.60 mm long. Dorsal fin arises around 2 mm from the junction of tail with body, shallow edge anteriorly, maximum height at mid posterior region of tail (Fig. 10B). Dorsal fin higher than ventral fin. Tail tip acuminate, not flagellated. Maximum tail height 2.44–2.69 mm. Width of tail musculature 35–50% of body width; height of tail musculature 59–77% of body height.

Oral disc positioned anteroventrally, laterally emarginate, oval in ventral view (Fig. 10B, C), 1.44–1.93 mm wide, and corresponding to 37–49% of body width at height of spiracle. Anterior labium with four short pyramidal papillae distributed in a single row and two papillae at each end of the labium (Fig. 10D, E). Posterior labium with a single row of 10–13 papillae, of which one or two are pyramidal at each end and the rest are cylindrical. Cylindrical papillae vary in size along the labium, being shorter at the ends and medially (Fig. 10D, E). Submar-

Table 5. Morphometric measurements in millimeters of 12 tadpoles of *Allobates albiventris* sp. nov., Gosner stages 34–37, from Manoel Urbano, Acre, Brazil. Values depict mean \pm standard deviation (range). Trait acronyms are defined in the text; n, sample size.

Traits	Stage 34 (n = 6)	Stage 35 (n = 1)	Stage 36 (n = 3)	Stage 37 (n = 2)
TL	17.14 \pm 0.48 (16.55–17.81)	17.72	19.26 \pm 0.13 (19.15–19.40)	20.03 \pm 0.06 (19.99–20.08)
TAL	11.61 \pm 0.38 (11.26–12.26)	12.10	13.13 \pm 0.05 (13.10–13.19)	13.69 \pm 0.00 (13.69–13.69)
BL	5.53 \pm 0.19 (5.29–5.80)	5.63	6.13 \pm 0.08 (6.05–6.22)	6.34 \pm 0.06 (6.30–6.38)
BW	3.85 \pm 0.36 (3.36–4.28)	4.12	3.53 \pm 0.08 (3.44–3.61)	4.03 \pm 0.24 (3.86–4.20)
BH	2.23 \pm 0.19 (1.93–2.44)	2.18	2.27 \pm 0.15 (2.10–2.35)	2.60 \pm 0.12 (2.52–2.69)
HWLE	3.19 \pm 0.21 (3.02–3.53)	3.70	3.02 \pm 0.00 (3.02–3.02)	3.40 \pm 0.06 (3.36–3.44)
TMW	1.55 \pm 0.09 (1.43–1.68)	1.43	1.51 \pm 0.08 (1.43–1.60)	1.64 \pm 0.18 (1.51–1.76)
MTH	2.58 \pm 0.09 (2.44–2.69)	2.69	2.80 \pm 0.10 (2.69–2.86)	2.94 \pm 0.12 (2.86–3.02)
TMH	1.54 \pm 0.10 (1.43–1.68)	1.51	1.62 \pm 0.05 (1.60–1.68)	1.68 \pm 0.00 (1.68–1.68)
IOD	0.99 \pm 0.35 (0.92–1.05)	1.01	1.04 \pm 0.05 (1.02–1.09)	1.13 \pm 0.06 (1.09–1.18)
IND	1.33 \pm 0.06 (1.26–1.43)	1.43	1.48 \pm 0.13 (1.34–1.60)	1.47 \pm 0.06 (1.43–1.51)
END	0.57 \pm 0.04 (0.50–0.63)	0.55	0.52 \pm 0.02 (0.50–0.55)	0.59 \pm 0.00 (0.59–0.59)
NSD	0.52 \pm 0.07 (0.42–0.63)	0.50	0.67 \pm 0.15 (0.50–0.80)	0.57 \pm 0.09 (0.50–0.63)
ED	0.82 \pm 0.04 (0.76–0.88)	0.84	0.91 \pm 0.06 (0.84–0.97)	0.92 \pm 0.00 (0.92–0.92)
SS	3.77 \pm 0.23 (3.36–4.03)	4.20	4.17 \pm 0.27 (3.86–4.37)	4.09 \pm 0.06 (4.03–4.12)
VTL	1.39 \pm 0.13 (1.23–1.60)	1.55	1.50 \pm 0.19 (1.36–1.71)	1.50 \pm 0.05 (1.46–1.53)
STL	0.55 \pm 0.07 (0.46–0.67)	0.42	0.55 \pm 0.04 (0.50–0.59)	0.67 \pm 0.06 (0.63–0.71)
ODW	1.67 \pm 0.18 (1.44–1.93)	1.53	1.46 \pm 0.14 (1.33–1.61)	1.76 \pm 0.23 (1.60–1.92)
PL	0.68 \pm 0.06 (0.59–0.74)	0.81	0.67 \pm 0.13 (0.52–0.76)	0.85 \pm 0.06 (0.81–0.89)
AL	0.48 \pm 0.03 (0.42–0.50)	0.50	0.62 \pm 0.03 (0.59–0.64)	0.59 \pm 0.07 (0.54–0.64)
DG	0.47 \pm 0.05 (0.40–0.54)	0.62	0.55 \pm 0.04 (0.50–0.59)	0.57 \pm 0.05 (0.54–0.60)
A1	1.16 \pm 0.05 (1.08–1.21)	1.14	1.13 \pm 0.07 (1.08–1.21)	1.23 \pm 0.06 (1.19–1.28)
A2	1.07 \pm 0.04 (1.01–1.11)	1.02	1.05 \pm 0.04 (1.01–1.09)	1.18 \pm 0.01 (1.18–1.19)
P1	1.02 \pm 0.11 (0.82–1.11)	0.99	1.01 \pm 0.10 (0.91–1.11)	1.19 \pm 0.00 (1.19–1.19)
P2	0.98 \pm 0.08 (0.82–1.08)	0.97	0.99 \pm 0.04 (0.94–1.02)	1.18 \pm 0.00 (1.18–1.18)
P3	0.67 \pm 0.14 (0.50–0.84)	0.49	0.49 \pm 0.04 (0.47–0.54)	0.76 \pm 0.04 (0.74–0.79)
UJW	0.67 \pm 0.00 (0.67–0.67)	0.67	0.56 \pm 0.10 (0.50–0.67)	0.67 \pm 0.00 (0.67–0.67)
UJL	0.74 \pm 0.05 (0.67–0.82)	0.94	0.81 \pm 0.04 (0.76–0.84)	0.77 \pm 0.07 (0.77–0.77)

ginal papillae absent. Upper jaw sheath arch-shaped, longer than lower jaw sheath and without median cut. Lower jaw V-shaped. Sheaths with serrations along their entire length. Labial formula of the keratodont row (LTRF) is 2(2)/3(1). Row A-1 measures 1.16 \pm 0.05 mm; A-2 measures 1.07 \pm 0.04 mm but is interrupted in the central region by a gap of approximately 40%. Row P-1 measures 1.02 \pm 0.11 mm, with a small medial gap. Rows P-2 and P-3 are complete; they measure 0.98 \pm 0.08 mm and 0.67 \pm 0.14 mm, respectively (Fig. 10D).

In preservative, body and tail muscles assume different shades of cream, with brown melanophores forming blotches and spots of various shapes and sizes. Fins cream but translucent, with brown spots of various shapes and sizes resembling a marbled pattern. Venter cream but translucent, with thickened brown melanophores mainly in the central region. Internal organs are visible through the skin (Fig. 10C).

Geographic distribution and natural history. *Allobates albiventris* sp. nov. is known from only five localities in southwestern Brazilian Amazonia: four in the State of Acre and one in the State of Amazonas (Figs 1 and 11). The species inhabits the leaf litter of primary and secondary ombrophilous forests at elevations between 125 and 184 m asl (Fig. 11). It has a diurnal habit and is general-

ly active between 0500 and 1800 h, with vocal activity peaks between 0500–0900 h and 1600–1800 h.

Allobates albiventris sp. nov. breeds in the rainy season between November and March. Males vocalize both on litterfall and while perched on shrubs or fallen branches up to 40 cm above ground (Fig. 8M). Clutches are deposited on the adaxial portion of living, attached leaves of small shrubs approximately 10–15 cm from the ground (Fig. 12F–H). We found eight egg clutches—three at the type locality (Manoel Urbano, Acre), four in Parque Ambiental Chico Mendes (Rio Branco, Acre) and one in Reserva Extrativista Arapixi (Boca do Acre, Amazonas). The number of eggs per clutch ranged from 17 to 31 (Fig. 12F, G). Two clutches were found on the same leaf (nest) (Fig. 12H). In freshly laid eggs, approximately half of the animal pole is darkly pigmented; the rest of the egg is white. The eggs are surrounded by an opaque, colloidal gel (Fig. 12F, G), which becomes denser and more opaque over the course of larval development.

Four mating pairs were observed in courtship, one at the type locality and three in Parque Ambiental Chico Mendes. Each observation began with the approach of a female to the perch where a male was emitting courtship calls. In each case, the male, perceiving the approach of a female, began to emit courtship calls interspersed with advertisement calls. He then jumped from the call perch

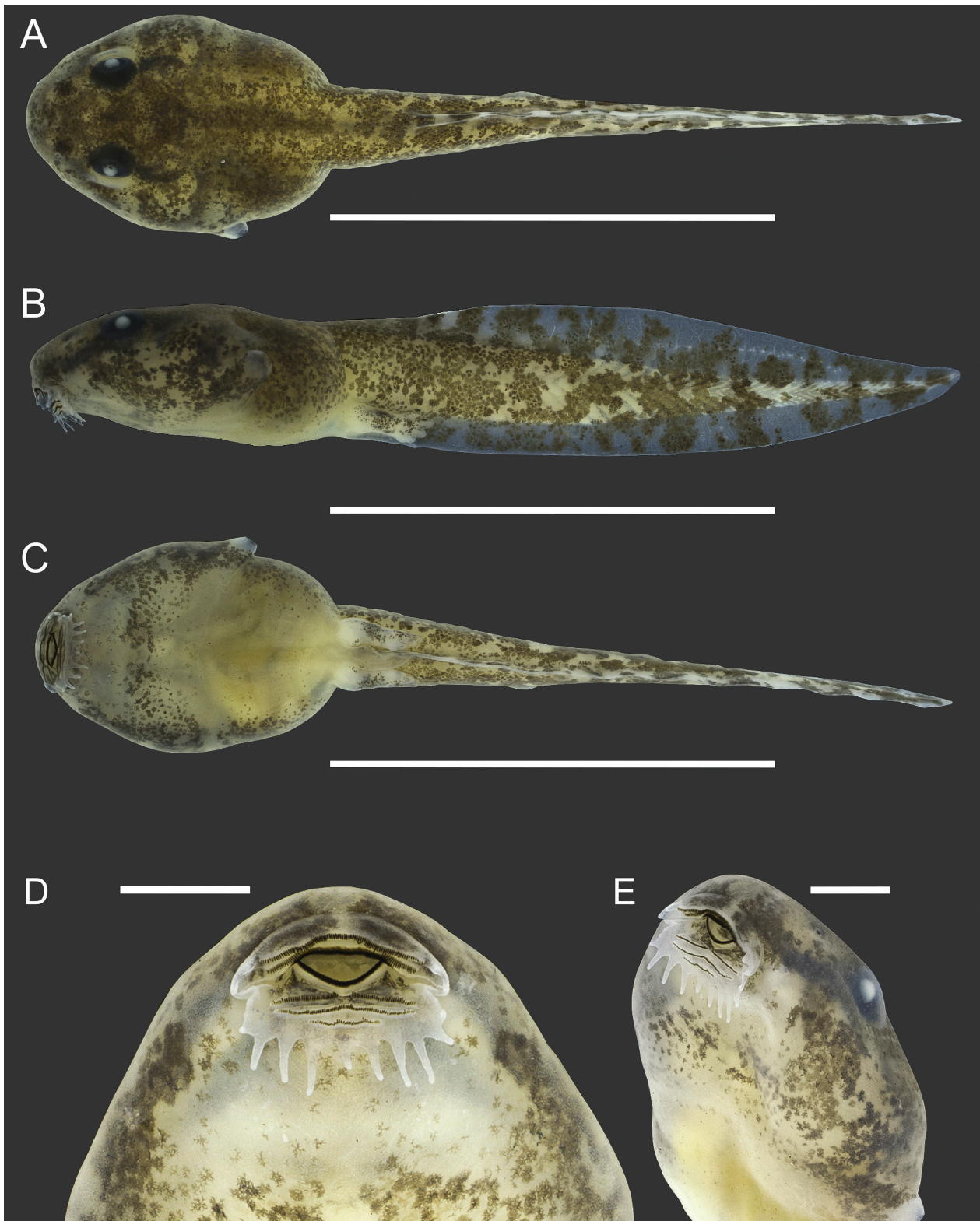


Figure 10. Preserved tadpole of *Allobates albiventris* sp. nov. (lot INPAH45066), Gosner stage 34. (A) Dorsal, (B) lateral and (C) ventrolateral views of the body, and (D) ventral and (E) ventrolateral views of the oral disc. Scale bar: 10 mm (A–C) and 1 mm (D, E). Photographs by J.R.D. Souza.

and attempted to guide the female (Fig. 12B) by conducting her to an oviposition site (bushes or seedlings) located up to 3 m from the perch. During the courtship march (sensu Rocha et al. 2018), which lasted between 3 and 5 min, the male continued to emit advertisement and courtship calls while the female sporadically made short stops.

Once arriving at the oviposition site, the male jumped to the adaxial surface of the leaf, located 10–15 cm from the ground, and continued vocalizing. The female followed the male and positioned herself underneath the leaf, at the edge closest to the ground. She then observed the male, raising her head toward the leaf. In all courtships, females

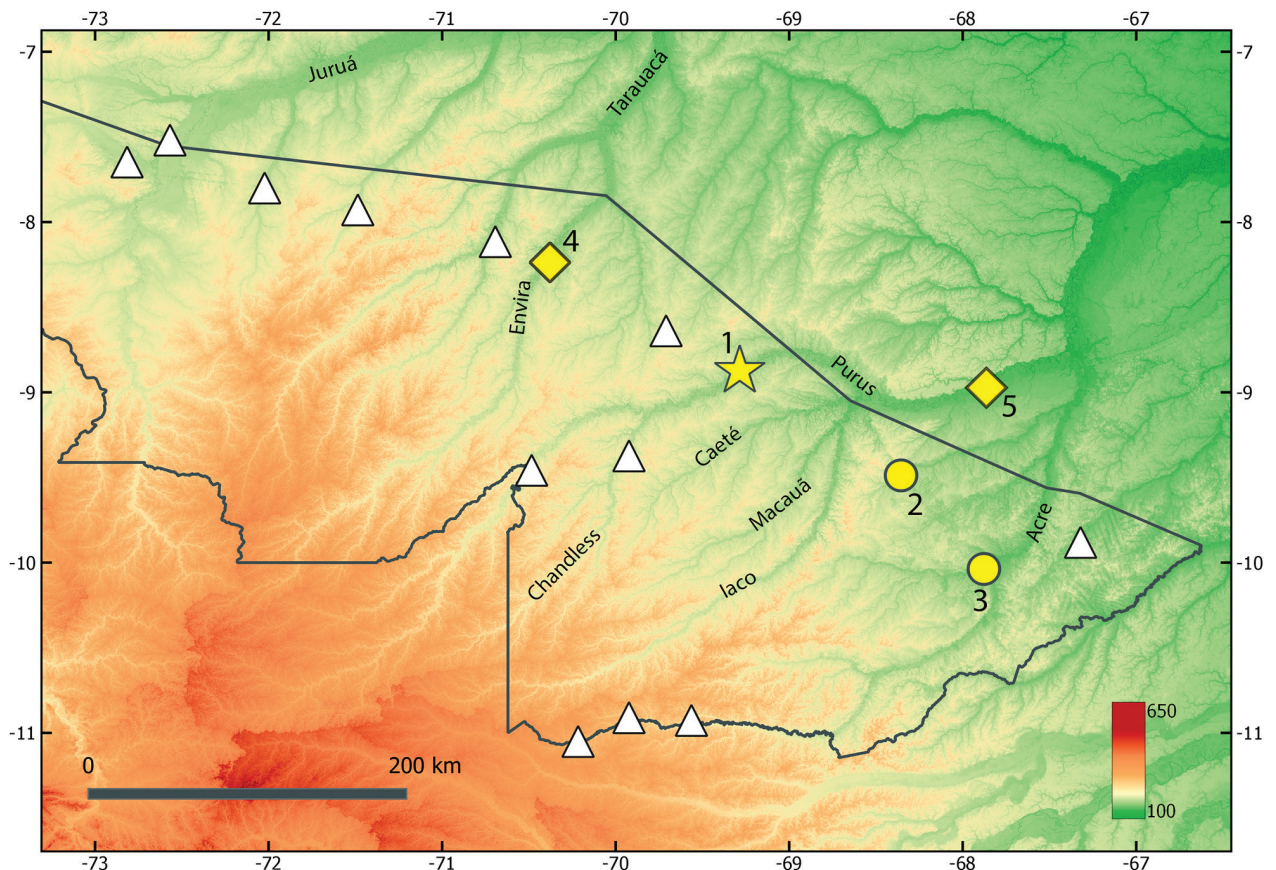


Figure 11. Geographic distribution of *Allobates albiventris* sp. nov. Star = type locality (1 Manoel Urbano); circles = additional paratype localities (2 Antimary River; 3 Parque Ambiental Chico Mendes); and rhombus (4 Feijó; 5 Reserva Extrativista Arapixi). White triangles denote sampled localities where the new species was not recorded.

positioned themselves vertically, with forelimbs only lightly touching the ground, for up to 1 min before jumping to the leaf (Fig. 12C). After the jump, the female approached the male. On one occasion, the female faced the male and put her snout on the male's pectoral region, then turned in the opposite direction. The male then climbed onto the female's back and they initiated amplexus (it was not possible to clearly discern the type of amplexus). In the other courtships, the female approached the male and quickly was grabbed by him. The male positioned himself laterally, snout to snout, and with one hand held the female's head, either by the region between the eyes and nostrils or directly on the snout (Fig. 12D). The resulting cephalic amplexus lasted from 1 to 4 min. During and after amplexus, a barely audible vocalization (similar to "cheeps"), was emitted by the male. Following amplexus, on one occasion the male quickly jumped into the leaf litter and returned to vocalize within 3 min. In the three other courtships, the male remained on the leaf while the female deposited eggs (Fig. 12E, H) but left the leaf before she finished. Two males initiated advertisement calls while the female was still ovipositing (Fig. 12H), while the third left the nest without vocalizing. On two occasions oviposition started with the male still in amplexus.

During oviposition, females repeatedly moved their heads upwards. This movement was interspersed with continuous clockwise or counterclockwise rotations relative to the vertical plane. Oviposition lasted ~11 to 15

min and ended when the female stopped the tilting motion with her head. However, she remained at the nest, on the clutch, and performed sporadic returns (apparently, hydrating the clutch, as her skin became excessively moist). Residence time of each female after oviposition ranged from 10 to 15 min, and the total time in the nest from 21 to 30 min. Males returned to the nest between 25 and 30 min after the female left, probably to hydrate the eggs and promote swelling of the surrounding jelly. We collected one clutch immediately after the female's departure, prior to the male's return, and the embryos developed normally. Only one male was observed performing larval transport (Fig. 12I).

Discussion

Nearly 10 years ago, Simões et al. (2013b) reported that nurse frogs from the middle Juruá and Ituxi rivers attributed to *Allobates gasconi* likely represent independent evolutionary lineages, a claim that was later corroborated by Vacher et al. (2020) through molecular delimitation methods. However, the absence of toptotypical genetic and bioacoustic data for *A. gasconi* sensu stricto hampered the subsequent taxonomic study of related taxa (Melo-Sampaio et al. 2018). Recently, Ferreira et al.



Figure 12. Habitat and natural history of *Allobates albiventris* sp. nov. **A** Typical understory of open ombrophilous forest at the type locality in Manoel Urbano, State of Acre, Brazil. **B** Beginning of courtship behavior, in which a male is leading a female to an oviposition site. **C** Female (unvouchered) positioning herself to jump to the adaxial surface of the leaf, where the male is vocalizing. **D** Mating pair (unvouchered) in cephalic amplexus. **E** Mating pair (unvouchered) on the leaf, with the female in oviposition and the male silent. **F** Recently deposited clutch, with the smallest clutch recorded (17 eggs). **G** The largest clutch recorded (31 eggs). **H** Mating pair on a leaf, where a male vocalizes while a female deposits a second clutch on the same leaf. **I** Male INPAH45045 carrying 10 tadpoles on his back. Photographs by J.R.D. Souza.

(2023) showed, based on topotypical data, that *A. gasconi* sensu stricto is not closely related to several populations previously assigned to it. *Allobates albiventris* is the first nominal species of this complex to be named and described. Since the name *A. gasconi* is not applicable to any population in this species complex, we instead refer to it as the *A. albiventris* species complex. The number of candidate species associated with *A. albiventris* differs among phylogenetic studies (Vacher et al. 2020; Réjaud et al. 2020; Ferreira et al. 2023; present study). However, molecular delimitation as presented here represents an initial attempt to delimit species, and we emphasize the need to further integrate morphologic, genetic and bio-

acoustic data to fully evaluate the cryptic diversity associated with *A. albiventris*.

Allobates albiventris is known from five lowland localities in southwestern Brazilian Amazonia. The species inhabits open ombrophilous forests dominated by bamboos of the genus *Guadua* and occupies pristine as well as secondary forests with low to moderate levels of anthropization (e.g., Parque Ambiental Chico Mendes and Reserva Extrativista Arapixi). Twelve additional localities, all at elevations above 300 m asl, were sampled in the upper Juruá and Purus river basins, but *A. albiventris* was only found below 200 m asl. We also surveyed seven permanent sampling modules along the upper Madei-

ra River, all < 200 m asl in open ombrophilous forests dominated by palms, but we found only *A. aff. albiventris* (*gasconi*) SL3 (Vacher et al. 2020). The geographic distribution of *A. albiventris* seems bounded on the east by the Acre River and on the west by the Envira River. Geographic distribution of other candidates in the *A. albiventris* complex remains poorly known since each is currently known from one or two localities (Appendix 3); further sampling in southwestern and central Amazonia is needed to clarify the range of each candidate and their limiting drivers.

Réjaud et al. (2020) suggest that modern large rivers promoted diversification of *Allobates* after the end of the Pebas system and that meandering rivers in western Brazilian Amazonia (e.g., Juruá and Purus rivers) may have played a modest role as biogeographic barriers, especially with respect to the diversification of early diverging species. Although the divergence time between *A. aff. albiventris* SL3 and the *A. tapajos* species complex is estimated at ~9.4 Mya (Réjaud et al. 2020), the divergence time among lineages of the *A. albiventris* species complex remains unknown. As this species complex is endemic to southwestern Amazonian lowlands and its distribution seems limited by small rivers and altitude, further biogeographic studies focused on its diversification may clarify the role of historical and geographical drivers in the speciation of this relatively ancient Amazonian frog complex.

Funding

This work was funded by the Brazilian Conselho Nacional de Desenvolvimento Científico e Tecnológico—CNPq (Universal grant no. 401120/2016-3 to APL), Brazilian Coordenação de Aperfeiçoamento de Pessoal de Nível Superior (CAPES) and Fundação de Amparo a Pesquisa do Estado do Amazonas—FAPEAM (BIODIVERSA Edital 007/2021, proc. 001760.2021-00). Miquéias Ferrão received an Edward O. Wilson Biodiversity Postdoctoral Fellowship from the Harvard Museum of Comparative Zoology and a fellowship from the David Rockefeller Center for Latin American Studies of Harvard University. Antonio Saulo Cunha Machado received a fellowship from FAPEAM (BIODIVERSA proc. 01.02.016301.03252/2021-67). Fieldwork in the Arapixi Extractive Reserve was supported by the Programa de Áreas Protegidas da Amazônia (ARPA), grant 010483/15. Paulo Roberto Melo-Sampaio received a fellowship from the Coordenação de Aperfeiçoamento de Pessoal de Nível Superior (CAPES; process 88882.183267/2018-01). Funders had no role in study design, data collection and analysis, decision to publish, or preparation of the manuscript.

Competing interests

The authors declare that they have no competing interests.

Acknowledgments

We thank Ana Prudente (MPEG), João F. M. Sarmento (MPEG), Fernanda P. Werneck (INPAH) and Ariane Silva (INPAH) for providing access to collections under their care; Luis Felipe Toledo and Simone

Dena for providing access to Fonoteca Neotropical Jacques Viellard; Valfredo C. Lima for logistic support; and Vinicius Guerra for helping with the advertisement call figure. Specimens were collected under permit number 1337-1 provided by the Instituto Brasileiro do Meio Ambiente e dos Recursos Naturais Renováveis (IBAMA) and by the Instituto Chico Mendes de Conservação da Biodiversidade (ICMBio). Protocols regarding animal collection and care follow Conselho Federal de Biologia resolution number 148/2012.

References

- Albert JS, Val P, Hoorn C (2018) The changing course of the Amazon River in the Neogene: Center stage for Neotropical diversification. *Neotropical Ichthyology* 16: e180033. <https://doi.org/10.1590/1982-0224-20180033>
- Altig R, McDiarmid RW (1999) Body plan: Development and morphology. In: McDiarmid RW, Altig R (Eds) *Tadpoles: The Biology of Anuran Larvae*. University of Chicago Press, Chicago, IL, 24–51.
- Baur H, Leuenberger C (2011) Analysis of ratios in multivariate morphometry. *Systematic Biology* 60: 813–825. <https://doi.org/10.1093/sysbio/syr061>
- Baur H, Leuenberger C (2020) Multivariate Ratio Analysis (MRA): R-scripts and tutorials for calculating Shape PCA, Ratio Spectra and LDA Ratio Extractor (1.05). Zenodo <https://doi.org/10.5281/zenodo.4250142>
- Benjamini Y, Hochberg Y (1995) Controlling the False Discovery Rate: A Practical and Powerful Approach to Multiple Testing. *Journal of the Royal Statistical Society. Series B (Methodological)* 57: 289–300. <http://www.jstor.org/stable/2346101>
- Bioacoustics Research Program (2015) Raven pro: Interactive sound analysis software, ver. 1.5. The Cornell Lab of Ornithology, Ithaca, NY.
- Bouckaert R, Vaughan TG, Barido-Sottani J, Duchêne S, Fourment M, Gavryushkina A, Heled J, Jones G, Kühnert D, de Maio N, Matschiner M, Mendes FK, Müller NF, Ogilvie HA, du Plessis L, Poppinga A, Rambaut A, Rasmussen D, Siveroni I, Suchard MA, Wu C, Xie D, Zhang C, Stadler T, Drummond AJ (2019) BEAST 2.5: An advanced software platform for Bayesian evolutionary analysis. *PLoS Computational Biology* 15: e1006650. <https://doi.org/10.1371/journal.pcbi.1006650>
- Boulenger GA (1884) On a collection of frogs from Yurimaguas, Hualaga River, Northern Peru. *Proceedings of the Zoological Society of London* 1883: 635–638. <https://doi.org/10.1111/j.1469-7998.1883.tb06669.x>
- Caldwell JP, Lima AP (2003) A new Amazonian species of *Colostethus* (Anura: Dendrobatidae) with a nidicolous tadpole. *Herpetologica* 59: 219–234. [https://doi.org/10.1655/0018-0831\(2003\)059\[0219:anasoc\]2.0.co;2](https://doi.org/10.1655/0018-0831(2003)059[0219:anasoc]2.0.co;2)
- Cavalcanti IRS, Luna MC, Faivovich J, Grant T (2022) Structure and evolution of the sexually dimorphic integumentary swelling on the hands of dendrobatid poison frogs and their relatives (Amphibia: Anura: Dendrobatoidea). *Journal of Anatomy* 240: 447–465. <https://doi.org/10.1111/joa.13569>
- Dubeux MJM, Nascimento FAC, Lima LR, Magalhães FM, Silva IRS, Golçalves U, Almeida JPF, Correia LL, Garda AA, Mesquita DO, Rossa-Feres DC, Mott T (2020) Morphological characterization and taxonomic key of tadpoles (Amphibia: Anura) from the northern region of the Atlantic forest. *Biota Neotropica* 20: e20180718. <https://doi.org/10.1590/1676-0611-BN-2018-0718>

- Ferrão M, Hanken J, Lima AP (2022) A new nurse frog of the *Allobates tapajos* species complex (Anura: Aromobatidae) from the upper Madeira River, Brazilian Amazonia. *PeerJ* 10: e13751. <https://doi.org/10.7717/peerj.13751>
- Ferreira AS, Ferrão M, Cunha-Machado AS, Magnusson WE, Hanken J, Lima AP (2023) Integrative reappraisal of the Amazonian nurse frog *Allobates gasconi* (Morales 2002) based on topotypical data, with implications for the systematics and taxonomy of a large species complex. *bioRxiv* 2023.07.10.548442. <https://doi.org/10.1101/2023.07.10.548442>
- Fernandes IY, Moraes LJCL, Menin M, Farias IP, Lima AP, Kaefer IL (2021) Unlinking the speciation steps: Geographical factors drive changes in sexual signals of an Amazonian nurse-frog through body size variation. *Evolutionary Biology* 48: 81–93. <https://doi.org/10.1007/s11692-020-09525-7>
- Fouquet A, Ferrão M, Jairam R (2023) Two new species of *Allobates* of the *trilineatus* clade (Anura: Aromobatidae) from the Eastern Guiana Shield. *Zootaxa* 5297: 533–561. <https://doi.org/10.11646/zootaxa.5297.4.4>
- Fox J, Weisberg S (2019) *An R Companion to Applied Regression*, Third edition. Sage, Thousand Oaks CA. Available at: <https://socialsciences.mcmaster.ca/jfox/Books/Companion>.
- Frost DR (2023) *Amphibian Species of the World: An Online Reference* (version 6.0). Available at <https://amphibiansoftheworld.amnh.org/index.php>. [Accessed 10May 2023.] American Museum of Natural History, New York, USA. <https://doi.org/10.5531/db.vz.0001>
- Fujisawa T, Barraclough TG (2013) Delimiting species using single-locus data and the generalized mixed yule coalescent approach: A revised method and evaluation on simulated data sets. *Systematic Biology* 62: 707–724. <https://doi.org/10.1093/sysbio/syt033>
- Gagliardi-Urrutia LAG, Castroviejo-Fisher S, Rojas-Runjaic FJM, Jaramillo-Martínez AF, Solís S, Simões PI (2021) A new species of nurse-frog (Aromobatidae, *Allobates*) from the Amazonian forest of Loreto, Peru. *Zootaxa* 5026: 375–404. <https://doi.org/10.11646/zootaxa.5026.3.3>
- Gosner KL (1960) A simplified table for staging anuran embryos and larvae with notes on identification. *Herpetologica* 16: 183–190. <https://www.jstor.org/stable/3890061>
- Grant T, Frost DR, Caldwell JP, Gagliardo R, Haddad CFB, Kok PJR, Means BD, Noonan BP, Schargel WE, Wheeler WC (2006) Phylogenetic systematics of dart-poison frogs and their relatives (Anura: Athesphatanura: Dendrobatidae). *Bulletin of the American Museum of Natural History* 299: 1–262. [https://doi.org/10.1206/0003-0090\(2006\)299\[1:psodfa\]2.0.co;2](https://doi.org/10.1206/0003-0090(2006)299[1:psodfa]2.0.co;2)
- Grant T, Rada M, Anganoy-Criollo M, Batista A, Dias PH, Jeckel AM, Machado DJ, Rueda-Almonacid JV (2017) Phylogenetic systematics of dart-poison frogs and their relatives revisited (Anura: Dendrobatoidea). *South American Journal of Herpetology* 12(S1): 1–90. <https://doi.org/10.2994/SAJH-D-17-00017.1>
- Grant T, Rodríguez LO (2001) Two new species of frogs of the genus *Colostethus* (Dendrobatidae) from Peru and a redescription of *C. trilineatus* (Boulenger, 1883). *American Museum Novitates* 3355: 1–24. <http://digitallibrary.amnh.org/handle/2246/2908>
- Hoang DT, Chernomor O, von Haeseler A, Minh BQ, Vinh LS (2018) UFBoot2: Improving the ultrafast bootstrap approximation. *Molecular Biology and Evolution* 35: 518–522. <https://doi.org/10.1093/molbev/msx281>
- Hudson RR (1990) Gene genealogies and the coalescent process. In: Futuyma DJ, Antonovics J (Eds) *Oxford Surveys in Evolutionary Biology*. Oxford University Press, Oxford, 1–44. http://home.uchicago.edu/~rhudson1/popgen356/OxfordSurveysEvolBiol7_1-44.pdf
- Jaramillo AF, Gagliardi-Urrutia G, Simões PI, Castroviejo-Fisher S (2021) Redescription and phylogenetics of *Allobates trilineatus* (Boulenger 1884 “1883”) (Anura: Aromobatidae) based on topotypic specimens. *Zootaxa* 4951: 201–235. <https://doi.org/10.11646/zootaxa.4951.2.1>
- Kaefer IL, Tsuji-Nishikido BM, Mota EP, Farias IP, Lima AP (2013) The early stages of speciation in Amazonian forest frogs: Phenotypic conservatism despite strong genetic structure. *Evolutionary Biology* 40: 228–245. <https://doi.org/10.1007/s11692-012-9205-4>
- Kalyaanamoorthy S, Minh B, Wong T, von Haeseler A, Jermiin LS (2017) ModelFinder: Fast model selection for accurate phylogenetic estimates. *Nature Methods* 14: 587–589. <https://doi.org/10.1038/nmeth.4285>
- Katoh K, Standley DM (2013) MAFFT multiple sequence alignment software version 7: Improvements in performance and usability. *Molecular Biology and Evolution* 30: 772–780. <https://doi.org/10.1093/molbev/mst010>
- Kearse M, Moir R, Wilson A, Stones-Havas S, Cheung M, Sturrock S, Buxton S, Cooper A, Markowitz S, Duran C, Thierer T, Ashton B, Meintjes P, Drummond A (2012) Geneious basic: An integrated and extendable desktop software platform for the organization and analysis of sequence data. *Bioinformatics* 28: 1647–1649. <https://doi.org/10.1093/bioinformatics/btts199>
- Kimura M (1980) A simple method for estimating evolutionary rates of base substitutions through comparative studies of nucleotide sequences. *Journal of Molecular Evolution* 16: 111–120. <https://doi.org/10.1007/bf01731581>
- Köhler J, Jansen M, Rodríguez A, Kok PJR, Toledo LF, Emmrich M, Glaw F, Haddad CFB, Rödel M-O, Vences M (2017) The use of bioacoustics in anuran taxonomy: Theory, terminology, methods and recommendations for best practice. *Zootaxa* 4251: 1–124. <https://doi.org/10.11646/zootaxa.4251.1.1>
- Lima AP, Caldwell JP (2001) A new Amazonian species of *Colostethus* with sky blue digits. *Herpetologica* 57: 133–138. <https://www.jstor.org/stable/3893182>
- Lima AP, Caldwell JP, Biavati G, Montanarin A (2010) A new species of *Allobates* (Anura: Aromobatidae) from Paleovárzea Forest in Amazonas, Brazil. *Zootaxa* 2337: 1–17. <https://doi.org/10.11646/zootaxa.2337.1.1>
- Lima AP, Ferrão M, Silva DL (2020) Not as widespread as thought: Integrative taxonomy reveals cryptic diversity in the Amazonian nurse frog *Allobates tinae* Melo-Sampaio, Oliveira & Prates, 2018 and description of a new species. *Journal of Zoological Systematics and Evolutionary Research* 58: 1173–1194. <https://doi.org/10.1111/jzs.12406>
- Lima AP, Sanchez DEA, Souza JRD (2007) A new Amazonian species of the frog genus *Colostethus* (Dendrobatidae) that lays its eggs on undersides of leaves. *Copeia* 2007: 114–122. [https://doi.org/10.1643/0045-8511\(2007\)7\[114:anasot\]2.0.co;2](https://doi.org/10.1643/0045-8511(2007)7[114:anasot]2.0.co;2)
- Lima AP, Simões PI, Kaefer IL (2014) A new species of *Allobates* (Anura: Aromobatidae) from the Tapajós River basin, Pará State, Brazil. *Zootaxa* 3889: 355–387. <https://doi.org/10.11646/zootaxa.3889.3.2>
- Lima AP, Simões PI, Kaefer IL (2015) A new species of *Allobates* (Anura: Aromobatidae) from Parque Nacional da Amazônia, Pará State, Brazil. *Zootaxa* 3980: 501–525. <https://doi.org/10.11646/zootaxa.3980.4.3>

- Maddison WP, Maddison DR (2015) Mesquite: A modular system for evolutionary analysis. Version 3.04. Available at <http://mesquite-project.org>.
- Maia GF, Lima AP, Kaefer IL (2017) Not just the river: Genes, shapes, and sounds reveal population-structured diversification in the Amazonian frog *Allobates tapajos* (Dendrobatoidea). *Biological Journal of the Linnean Society* 121: 95–108. <https://doi.org/10.1093/biolinnean/blw017>
- Melo-Sampaio PR, Oliveira RM, Prates I (2018) A new nurse frog from Brazil (Aromobatidae: *Allobates*) with data on the distribution and phenotypic variation of western Amazonian species. *South American Journal of Herpetology* 13: 131–149. <https://doi.org/10.2994/sajh-d-17-00098.1>
- Melo-Sampaio PR, Prates I, Peloso PLV, Recoder R, Dal Vechio F, Marques-Souza S, Rodrigues MT (2020) A new nurse frog from Southwestern Amazonian highlands, with notes on the phylogenetic affinities of *Allobates alessandroi* (Aromobatidae). *Journal of Natural History* 54: 43–62. <https://doi.org/10.1080/00222933.2020.1727972>
- Melo-Sampaio PR, Souza MB, Peloso PLV (2013) A new riparian species of *Allobates* Zimmermann and Zimmermann, 1988 (Anura: Aromobatidae) from southwestern Amazonia. *Zootaxa* 3716: 336–348. <https://doi.org/10.11646/zootaxa.3716.3.2>
- Moraes LJCL, Lima AP (2021) A new nurse frog (*Allobates*, Aromobatidae) with a cricket-like advertisement call from eastern Amazonia. *Herpetologica* 77: 146–163. <https://doi.org/10.1655/Herpetologica-D-20-00010.1>
- Moraes LJCL, Pavan D, Lima AP (2019) A new nurse frog of *Allobates masniger-nidicola* complex (Anura, Aromobatidae) from the east bank of Tapajós River, eastern Amazonia. *Zootaxa* 4648: 401–434. <https://doi.org/10.11646/zootaxa.4648.3.1>
- Morales VR (2002) Sistemática y biogeografía del grupo *trilineatus* (Amphibia, Anura, Dendrobatidae, *Colostethus*), con descripción de once especies nuevas. *Publicaciones de La Asociación de Amigos de Doñana* 13: 1–59.
- Nguyen LT, Schmidt HA, von Haeseler A, Minh BQ (2015) IQ-TREE: A fast and effective stochastic algorithm for estimating maximum-likelihood phylogenies. *Molecular Biology and Evolution* 32: 268–274. <https://doi.org/10.1093/molbev/msu300>
- Nunes-de-Almeida CHL, Haddad CFB, Toledo LF (2021) A revised classification of the amphibian reproductive modes. *Salamandra* 57: 413–427.
- Palumbi SR (1996) Nucleic acids II: The polymerase chain reaction. In: Hillis DM, Moritz C, Mable BK (Eds) *Molecular Systematics*. Sinauer & Associates, Sunderland, MA, 205–247.
- Pons J, Barraclough TG, Gomez-Zurita J, Cardoso A, Duran DP, Hazell S, Kamoun S, Sumlin WD, Vogler AP (2006) Sequence-based species delimitation for the DNA taxonomy of undescribed insects. *Systematic Biology* 55: 595–609. <https://doi.org/10.1080/106351-50600852011>
- Puillandre N, Brouillet S, Achaz G (2021) ASAP: Assemble species by automatic partitioning. *Molecular Ecology Resources* 21: 609–620. <https://doi.org/10.1111/1755-0998.13281>
- Puillandre N, Lambert A, Brouillet S, Achaz G (2012) ABGD, Automatic Barcode Gap Discovery for primary species delimitation. *Molecular Ecology* 21: 1864–1877. <https://doi.org/10.1111/j.1365-294x.2011.05239.x>
- R Core Team (2021) R: A language and environment for statistical computing. R Foundation for Statistical Computing, Vienna. Available online at <https://www.R-project.org>.
- Rambaut A, Drummond AJ, Xie D, Baele G, Suchard MA (2018) Posterior summarization in Bayesian phylogenetics using Tracer 1.7. *Systematic Biology* 67: 901. <https://doi.org/10.1093/sysbio/syy032>
- Randrianiaina RD, Strauß A, Glos F, Glaw F, Vences M (2011) Diversity, external morphology and ‘reverse taxonomy’ in the specialized tadpoles of Malagasy river bank frogs of the subgenus *Ochthomantis* (genus *Mantidactylus*). *Contributions to Zoology* 80: 17–65. <https://doi.org/10.1163/18759866-08001002>
- Réjaud A, Rodrigues MT, Crawford AJ, Castroviejo-Fisher S, Jaramillo AF, Chaparro JC, Glaw F, Gagliardi-Urrutia G, Moravec J, De la Riva I, Perez P, Lima AP, Werneck FP, Hrbek T, Ron SR, Ernst R, Kok PJR, Driskell A, Chave J, Fouquet A (2020) Historical biogeography identifies a possible role of Miocene wetlands in the diversification of the Amazonian rocket frogs (Aromobatidae: *Allobates*). *Journal of Biogeography* 47: 2472–2482. <https://doi.org/10.1111/jbi.13937>
- Rocha SMC, Lima AP, Kaefer IL (2018) Territory size as a main driver of male-mating success in an Amazonian nurse frog (*Allobates paleovarzensis*, Dendrobatoidea). *Acta Ethologica* 21: 51–57. <http://dx.doi.org/10.1007/s10211-017-0280-5>
- Santos JC, Coloma LA, Summers K, Caldwell JP, Ree R, Cannatella DC (2009) Amazonian amphibian diversity is primarily derived from Late Miocene Andean lineages. *PLoS Biology* 7: 1–14. <https://doi.org/10.1371/journal.pbio.1000056>
- Schulze A, Jansen M, Köhler G (2015) Tadpole diversity of Bolivia’s lowland anuran communities: molecular identification, morphological characterization, and ecological assignment. *Zootaxa* 4016: 1–111. <https://doi.org/10.11646/zootaxa.4016.1.1>
- Silva LA, Marques R, Folly H, Santana DJ (2022) A new Amazonian species of *Allobates* Zimmermann & Zimmermann, 1988 (Aromobatidae) with a trilled advertisement call. *PeerJ* 10: 113026. <https://doi.org/10.7717/peerj.13026>
- Simões PI, Gagliardi-Urrutia LAG, Rojas-Runjaic FJM, Castroviejo-Fisher S (2018) A new species of nurse-frog (Aromobatidae, *Allobates*) from the Juami River basin, northwestern Brazilian Amazonia. *Zootaxa* 4387: 109–133. <https://doi.org/10.11646/zootaxa.4083.4.3>
- Simões PI, Sturaro MJ, Peloso PLV, Lima AP (2013a) A new diminutive species of *Allobates* Zimmermann and Zimmermann, 1988 (Anura, Aromobatidae) from the northwestern Rio Madeira/Rio Tapajós interfluvie, Amazonas, Brazil. *Zootaxa* 3609: 251–273. <https://doi.org/10.11646/zootaxa.3609.3.1>
- Simões PI, Kaefer IL, Farias IP, Lima AP (2013b) An integrative appraisal of the diagnosis and distribution of *Allobates sumtuosus* (Morales, 2002) (Anura, Aromobatidae). *Zootaxa* 3746: 401–421. <https://doi.org/10.11646/zootaxa.3746.3.1>
- Simões PI, Rojas D, Lima AP (2019) A name for the nurse-frog (*Allobates*, Aromobatidae) of Floresta Nacional de Carajás, Eastern Brazilian Amazonia. *Zootaxa* 4550: 71–100. <https://doi.org/10.11646/zootaxa.4550.1.3>
- Souza JRD, Ferrão M, Hanken J, Lima AP (2020) A new nurse frog (Anura: *Allobates*) from Brazilian Amazonia with a remarkably fast multi-noted advertisement call. *PeerJ* 8: e9979. <https://doi.org/10.7717/peerj.9979>
- Sueur J, Aubin T, Simonis C (2008) Seewave, a free modular tool for sound analysis and synthesis. *Bioacoustics* 18: 213–226. <https://doi.org/10.1080/09524622.2008.9753600>
- Tamura K, Stecher G, Kumar S (2021) MEGA11: Molecular Evolutionary Genetics Analysis version 11. *Molecular Biology and Evolution* 38: 3022–3027. <https://doi.org/10.1093/molbev/msab120>

Vacher J-P, Chave J, Ficetola FG, Sommeria-Klein G, Tao S, Thébaud C, Blanc M, Camacho A, Cassimiro J, Colston TJ, Dewynter M, Ernst R, Gaucher P, Gomes JO, Jairam R, Kok PJR, Lima JD, Martinez Q, Marty C, Noonan BP, Nunes PMS, Ouboter P, Recoder R, Rodrigues MT, Snyder A, Souza SM, Fouquet A (2020) Large-scale DNA-based survey of frogs in Amazonia suggests a vast underesti-

ation of species richness and endemism. *Journal of Biogeography* 47: 1781–1791. <https://doi.org/10.1111/jbi.13847>

Zimmermann H, Zimmermann E (1988) Etho-Taxonomie und zoogeographische Artengruppenbildung bei Pfeilgiftfröschen (Anura: Dendrobatidae). *Salamandra* 24: 125–160.

Appendix 1

Species, museum voucher specimens and GenBank accession numbers of sequences used in molecular analyses. Accession numbers in bold font denote sequences generated in the present study.

Species	Voucher	12S	16S	ND1	COI	cyt b
<i>Allobates</i> aff. <i>granti</i>	I2SPG	JN690205	JN690931			
<i>A.</i> aff. <i>magnussoni</i>	977126	MT627173	MT627173	MT627173	MT627173	MT627173
<i>A.</i> aff. <i>melanolaemus</i>	MTR28013	MT627203	MT627203	MT627203	MT627203	MT627203
<i>A.</i> aff. <i>olfersioides</i> 1	MTR17821		KDQF01003353			
<i>A.</i> aff. <i>olfersioides</i> 2	MTR16435	MT627202	MT627202	MT627202	MT627202	MT627202
<i>A.</i> aff. <i>olfersioides</i> 3	JFT959		KDQF01002701			
<i>A.</i> aff. <i>tapajos</i> 1	MTR10084	MT627197	MT627197	MT627197	MT627197	MT627197
<i>A.</i> aff. <i>tapajos</i> 2	AF1906	MT627175	MT627175	MT627175	MT627175	MT627175
<i>A.</i> aff. <i>tinae</i> 1	MPEG13397	DQ502213	DQ502213		DQ502900	DQ502648
<i>A.</i> aff. <i>trilineatus</i> 1	FGZC3247	MT627185	MT627185	MT627185	MT627185	MT627185
<i>A.</i> aff. <i>trilineatus</i> 2	JMP2313	MT627195	MT627195	MT627195	MT627195	MT627195
<i>A.</i> aff. <i>undulatus</i>	AMNHA159139	DQ283044	DQ283044		DQ502756	DQ502459
<i>A. algorei</i>	TNHCFSS551	HQ290950	HQ290950	HQ290950		HQ290530
<i>A. amissibilis</i>	PK3798	MT627204	MT627204	MT627204	MT627204	MT627204
<i>A. bacurau</i>	INPAH35401		KU195701			
<i>A. caeruleodactylus</i>	MTR10227	MT627199	MT627199	MT627199	MT627199	MT627199
<i>A. caldwella</i>	MPEG13826	DQ502099	DQ502099			DQ502531
<i>A. carajas</i>	BM163	MT627183	MT627183	MT627183	MT627183	MT627183
<i>A. chalcopis</i>	Alca1	MT627182	MT627182	MT627182	MT627182	
<i>A. albiventris</i> sp. nov.	MCP13630		KY886577			KY886618
<i>A. albiventris</i> sp. nov.	MNRJ91665		KY886576			KY886617
<i>A. albiventris</i> sp. nov.	MNRJ91679		KY886578			KY886619
<i>A. albiventris</i> sp. nov.	MNRJ91683		KY886574			KY886615
<i>A. albiventris</i> sp. nov.	MNRJ91684		KY886575			KY886616
<i>A. albiventris</i> sp. nov.	INPAH45061		ON937753			
<i>A. albiventris</i> sp. nov.	INPAH45060		ON937752			
<i>A. albiventris</i> sp. nov.	INPAH45064		ON937746			
<i>A. albiventris</i> sp. nov.	INPAH45065		ON937745			
<i>A. albiventris</i> sp. nov.	INPAH45048		ON937748			
<i>A. albiventris</i> sp. nov.	INPAH45044		ON937749			
<i>A. albiventris</i> sp. nov.	INPAH45035		ON937750			
<i>A. albiventris</i> sp. nov.	INPAH45051		ON937751			
<i>A. albiventris</i> sp. nov.	INPAH45040		ON937747			
<i>A. conspicuus/subfolioidificans</i>	FGZC3279	MT627186	MT627186	MT627186	MT627186	MT627186
<i>A. crombiei</i>	AF1097	MT627174	MT627174	MT627174	MT627174	MT627174
<i>A. femoralis</i>	AF3224	MT627179	MT627179	MT627179	MT627179	MT627179
<i>A. femoralis</i> SS	AfemShucv3a	DQ523001	DQ523072			DQ523142
<i>A. flaviventris</i>	HJ545	MT627192	MT627192	MT627192	MT627192	MT627192
<i>A. fratisenescus</i>	QCAZ54377		MF624172			MF614174
<i>A. gasconi</i> sensu stricto	GGU684		MT524137			
<i>A. gasconi</i> sensu stricto	APL23345		ON997555			
<i>A. gasconi</i> sensu stricto	APL23342		ON997554			
<i>A. gasconi</i> sensu stricto	APL23346		ON997547			
<i>A. gasconi</i> sensu stricto	APL23354		ON997552			

Species	Voucher	12S	16S	ND1	COI	cyt b
<i>A. gasconi</i> sensu stricto	APL23411		ON997558			
<i>A. aff. albiventris</i> SL1	APL14410		KJ747333			
<i>A. aff. albiventris</i> SL1	APL14411		KJ747334			
<i>A. aff. albiventris</i> SL1	APL14416		KJ747335			
<i>A. aff. albiventris</i> SL2	APL23940		OQ297604			
<i>A. aff. albiventris</i> SL2	APL24058		OQ297605			
<i>A. aff. albiventris</i> SL2	APL24068		OQ297606			
<i>A. aff. albiventris</i> SL2	APL24070		OQ297607			
<i>A. aff. albiventris</i> SL2	APL24071		OQ297608			
<i>A. aff. albiventris</i> SL3	HJ480	MT627191	MT627191	MT627191	MT627191	MT627191
<i>A. aff. albiventris</i> SL3	HJ299		KDQF01002640			
<i>A. aff. albiventris</i> SL5	MNRJ 91681		KY886572			
<i>A. aff. albiventris</i> SL5	MNRJ 91682		KY886573			KY886614
<i>A. aff. albiventris</i> SL5	OMNH36636	DQ502209	DQ502209		DQ502898	DQ502644
<i>A. aff. albiventris</i> SL5	MPEG13003	DQ502052	DQ502052		DQ502777	DQ502483
<i>A. aff. albiventris</i> SL5	MNRJ 90229		KY886570			KY886612
<i>A. aff. albiventris</i> SL5	MNRJ 90230		KY886571			KY886613
<i>A. goianus</i>	SAMA8574	MT627207	MT627207	MT627207	MT627207	MT627207
<i>A. granti</i>	AF1998	MT627176	MT627176	MT627176	MT627176	MT627176
<i>A. grillicantus</i>	MPEG43046		MW220039			
<i>A. grillisimilis</i>	MTR12749	MT627200	MT627200	MT627200	MT627200	MT627200
<i>A. hodli</i>	ABU2194		KX044279			
<i>A. humilis/pittieri</i>	CVULA5690	KJ940454	KJ940454			
<i>A. insperatus/juami</i>	JMP1703	MT627193	MT627193	MT627193	MT627193	MT627193
<i>A. juanii/ranooides</i>	ARA2394	DQ502271	DQ502271		DQ502933	DQ502702
<i>A. kamilae</i>	HJ285	MT627189	MT627189	MT627189	MT627189	MT627189
<i>A. kingsburyi</i>	QCAZ16523	AY364549	HQ290963			HQ290541
<i>A. magnussoni</i>	BM168	MT627184	MT627184	MT627184	MT627184	MT627184
<i>A. marchesianus</i>	AJC2498	MT627180	MT627180	MT627180	MT627180	MT627180
<i>A. masniger</i>	MTR10155	MT627198	MT627198	MT627198	MT627198	MT627198
<i>A. melanolaemus</i>	NMP6V711404		MT524148			
<i>A. nidicola</i>	MPEG13821	DQ502101	DQ502101			DQ502533
<i>A. niputidea</i>	MUJ3520	DQ502272	DQ502272		DQ502934	DQ502703
<i>A. nunciatus</i>	MPEG36777	MT627196	MT627196	MT627196	MT627196	MT627196
<i>A. olfersioides</i>	MNRJ79897	MF624178	MF624178			MF614175
<i>A. ornatus</i>	MHNSM22863		EU342550			
<i>A. pacaas</i>	MZUSP158938		MT076999			
<i>A. paleovarzensis</i>	JMP2196	MT627194	MT627194	MT627194	MT627194	
<i>A. sieggreenae</i>	MCP14533		MW293942			
<i>A. sp. Huanuco</i>	FGZC3348	MT627187	MT627187	MT627187	MT627187	MT627187
<i>A. sp. Neblina</i>	MTR15537	MT627201	MT627201	MT627201	MT627201	MT627201
<i>A. sumtuosus</i>	AF2212	MT627177	MT627177	MT627177	MT627177	MT627177
<i>A. talamancae</i>	QCAZ35236	MT627205	MT627205	MT627205	MT627205	MT627205
<i>A. tapajos</i>	MJH3973	DQ502110	DQ502110		DQ502820	DQ502542
<i>A. tinae</i>	HJ298	MT627190	MT627190	MT627190	MT627190	MT627190
<i>A. trilineatus</i>	AF4493		MT524111			
<i>A. undulatus</i>	AJC3040	MT627181	MT627181	MT627181	MT627181	MT627181
<i>A. velocicantus</i>	MCP10187/88	MF624181	MF624181			MF614178
<i>A. zaparo</i>	USNM546405	DQ502026	DQ502026		DQ502752	DQ502455
<i>Ameerega hahneli</i>	AF2673	MT627178	MT627178	MT627178	MT627178	MT627178
<i>Anomaloglossus stepheni</i>	MJH3928	DQ502107	DQ502107		DQ502818	DQ502539
<i>Aromobates saltuensis/</i> <i>nocturnus</i>	TNHCF5541/ AMNHA130042	HQ290970	HQ290970	HQ290970	DQ502860	DQ502592
<i>Colostethus brachistriatus</i>	CZPDUV4603	MF624204	MF624204		MF614304	MF614198
<i>Dendrobates auratus</i>	MVZHerp149723	JX564862	JX564862	JX564862	JX564862	JX564862
<i>Epipedobates boulengeri</i>	UMMZ227952/ QCAZ16574	HQ290997	HQ290997	HQ290997	DQ502742	DQ502447
<i>Leucostethus fugax</i>	QCAZ16513	HQ290958	HQ290958	HQ290958		HQ290538
<i>Mannophryne collaris</i>	FS5523	MT627188	MT627188	MT627188	MT627188	MT627188

Species	Voucher	I2S	I6S	ND1	COI	cyt b
<i>Phyllobates terribilis</i>	TNHC64420/ AMNHA118566	HQ291006	HQ291006	HQ291006	DQ502861	DQ502593
<i>Rheobates palmatus</i>	RHEOPALM	MT627206	MT627206	MT627206	MT627206	MT627206
<i>Silverstoneia nubicola/erasmios</i>	TNHCFS4942/ MAR336	HQ290966	HQ290966	HQ290966	MF614333	MF614237

Appendix 2

Specimens examined. Acronyms: **INPAH**, Herpetological Collection of the Instituto Nacional de Pesquisas da Amazônia, Manaus, Amazonas, Brazil; **MNRJ**, Museu Nacional do Rio de Janeiro, Rio de Janeiro, Brazil; **MPEG**, Herpetological Collection of the Museu Paraense Emílio Goeldi, Belém, Pará, Brazil; **MZUSP**, Museu de Zoologia, Universidade de São Paulo, São Paulo, Brazil. **UFAC-RB**, Herpetological Collection of the Universidade Federal do Acre, Rio Branco, Acre, Brazil.

Allobates caeruleodactylus. Adults. Brazil: Amazonas: km 12 on the road to Autazes (INPAH 7238 [holotype]; 7229–32, 7234–37 [paratypes]). Tadpoles. Brazil: Amazonas: km 12 on the road to Autazes [lots INPAH 8037–46, 8085].

Allobates flaviventris. Adults. Brazil: Acre: Senador Guimard, Fazenda Bonal (UFAC-RB 4650 [holotype], 4599–4601, 4603, 4631–35, 4675–77 [paratypes]).

Allobates fuscillus. Adults. Brazil: Amazonas: Juruá River: Penedo (INPAH 2532 [holotype], 2312, 2333, 2351, 2531, 2534, 2537 [paratypes]), Jainu (INPAH 3114, 3127, 3250, 3270, 3514 [paratypes]).

Allobates gasconi. Adults. Brazil: Amazonas: Jainu, west bank of Juruá River (INPAH 3082 [holotype]; 3079, 3083–84, 3090, 3093, 3249, 3412, 3483, 3491, 3494, 3512–13 [paratypes]).

Allobates grillicantus. Adults. Brazil: Pará: Trairão (MPEG 43046 [holotype]; 43038–41, 43045, 43047–50 [paratypes]); km 24 on Brazilian federal highway BR-163 (INPAH 41352–56 [paratypes]). Tadpoles. Brazil: Pará: Trairão (lots MPEG 43051–53, INPAH 41357).

Allobates grillisimilis. Adults. Brazil: Amazonas: Borba (INPAH 30779 [holotype]; 30780–808 [paratypes]); Nova Olinda do Norte (INPAH 30809–23 [paratypes]).

Allobates nidicola. Adults. Brazil: Amazonas: km 12 on road to Autazes (INPAH 8093 [holotype]; 7253–59, 7261–62, 8094 [paratypes]; 28122, 28124, 28127, 28129, 28131, 28144, 28159, 28163, 28166, 28169, 28171–72, 28174, 28179, 28184–85 [topotypes]). Tadpoles. Brazil: Amazonas: km 12 on road to Autazes (lots INPAH 8021–33, 8137–39).

Allobates pacaas. Adults. Brazil: Rondônia: Parque Nacional dos Pacaás Novos (MZUSP 158934 [holotype], 158935–38, MNRJ 93128–29, MPEG 42818–19, UFAC-RB 9470 [paratypes]).

Allobates paleovarzensis. Adults. Brazil: Amazonas: Careiro da Várzea (INPAH 20904 [holotype]; 20861–903, 20905 [paratypes]).

Allobates subfolionidificans. Adults. Brazil: Acre: Rio Branco, Parque Zoobotânico da Universidade Federal do Acre (INPAH 13760 [holotype], 11959–74, 13749–54 [paratypes]). Tadpoles. Brazil: Acre: Rio Branco, Parque Zoobotânico da Universidade Federal do Acre (lots INPAH 14822, 14823).

Allobates tapajos. Adults. Brazil: Pará: Parque Nacional da Amazônia (INPAH 34425 [holotype]; 34402–24 [paratypes]). Tadpoles. Brazil: Pará: Parque Nacional da Amazônia (lots INPAH 34426–27).

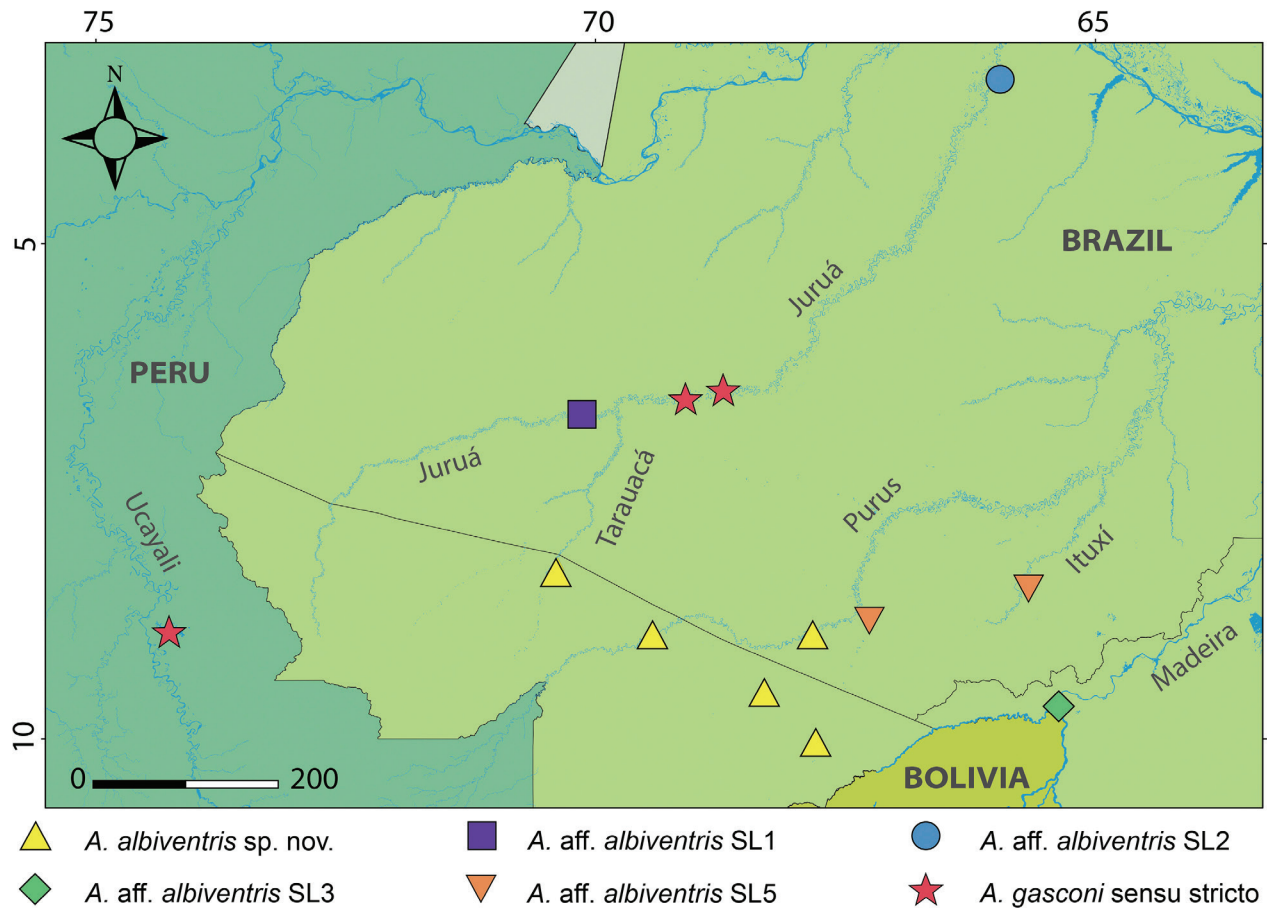
Allobates tinae. Adults. Brazil: Rondônia: Porto Velho, west bank of upper Madeira River (INPAH 41012–21, 41029–36, 41041–44); Amazonas: Boca do Acre (INPAH 40976, 41022, 41027, 41037, 41040; MNRJ 90214 [holotype], 90215–28, [paratypes]; UFAC-RB 4625 [paratype]); Acre: Senador Guimard (UFAC-RB 4604, 4636–37 [paratypes]).

Allobates trilineatus. Adults. Brazil: Acre: Rio Branco, Parque Zoobotânico of Universidade Federal do Acre (INPAH 11958–93)

Allobates vanzolinus. Adults. Brazil: Amazonas: Juruá River, Vai-Quem-Quer (INPAH 4896 [holotype]; 4903–05, 4912 [paratypes]); Jainu, Rio Juruá (INPAH 3381, 3413 [paratypes]).

Allobates velocantus. Adults. Brazil: Acre: Mâncio Lima (INPAH 41342 [holotype], 41338–41, 41344–48 [paratypes]). Tadpoles. Brazil: Acre: Mâncio Lima (lot INPAH 41351).

Appendix 3



Geographic distribution of samples of *Allobates gasconi* and *A. albiventris* species complex included in the phylogenetic analyses. Lineage numbering (SL) follows those of Figure 2.

Supplementary Material 1

Table S1

Authors: Souza JRD, Ferrão M, Kaefer IL, Cunha-Machado AS, Melo-Sampaio PR, Hanken J, Lima AP (2023)

Data type: .xlsx

Explanation note: Morphometric measurements of *Allobates albiventris* **sp. nov.** and *A. gasconi*.

Copyright notice: This dataset is made available under the Open Database License (<http://opendatacommons.org/licenses/odbl/1.0>). The Open Database License (ODbL) is a license agreement intended to allow users to freely share, modify, and use this dataset while maintaining this same freedom for others, provided that the original source and author(s) are credited.

Link: <https://doi.org/10.3897/vz.73.e103534.suppl1>

Supplementary Material 2

Table S2

Authors: Souza JRD, Ferrão M, Kaefer IL, Cunha-Machado AS, Melo-Sampaio PR, Hanken J, Lima AP (2023)

Data type: .xlsx

Explanation note: Morphometric measurements of tadpoles of *Allobates albiventris* **sp. nov.**

Copyright notice: This dataset is made available under the Open Database License (<http://opendatacommons.org/licenses/odbl/1.0>). The Open Database License (ODbL) is a license agreement intended to allow users to freely share, modify, and use this dataset while maintaining this same freedom for others, provided that the original source and author(s) are credited.

Link: <https://doi.org/10.3897/vz.73.e103534.suppl2>

Supplementary Material 3

Figure S1

Authors: Souza JRD, Ferrão M, Kaefer IL, Cunha-Machado AS, Melo-Sampaio PR, Hanken J, Lima AP (2023)

Data type: .png

Explanation note: Maximum likelihood phylogenetic tree of *Allobates* based on five mitochondrial genes (12S, 16S, COI, ND1 and cyt b).

Copyright notice: This dataset is made available under the Open Database License (<http://opendatacommons.org/licenses/odbl/1.0>). The Open Database License (ODbL) is a license agreement intended to allow users to freely share, modify, and use this dataset while maintaining this same freedom for others, provided that the original source and author(s) are credited.

Link: <https://doi.org/10.3897/vz.73.e103534.suppl3>